LUNFD6/(NFFL-7175) 1999
27 October 1999

# BEAUTY'99 Conference Summary

Paula Eerola [1]
*Lund University, Lund, Sweden*



## Abstract

Investigations of B hadrons are expected to break new ground in measuring CP-violation effects. This series of BEAUTY conferences, originating from the 1993 conference in Liblice, has contributed significantly in developing ideas of CP-violation measurements using B hadrons and formulating and comparing critically the B-physics experiments. In the '99 conference in Bled we saw the ripening of the field and the first fruit emerging – Tevatron have produced beautiful B-physics results and more are expected to come with the next run, while the B-physics experiments at DESY, SLAC and KEK are starting their operation. The longer-term projects at LHC and Tevatron have taken their shape and detailed prototyping work is going on. Meanwhile, on the phenomenological side, there has been impressive theoretical progress in understanding deeper the 'standard' measurements and proposing new signatures. In this summary, I will highlight the status of the field as presented in the conference, concentrating on signatures, experiments, and R&D programmes.

[1] paula.eerola@quark.lu.se

# 1 Introduction

CP violation is a key phenomenon in elementary particle physics for completing our present understanding of particles and interactions, formulated by the Standard Model of electroweak interactions, and searching for inconsistencies indicating effects from physics beyond the Standard Model. Investigations of B hadrons are expected to break new ground in measuring CP violation effects.

CP violation can occur in any theory in which there are complex coefficients in the Lagrangian. In the Standard Model (SM), the origin of the CP violation is the complex coupling of quarks to the Higgs field. After the electroweak symmetry breaking, and after removing unphysical phases, one irremovable complex phase remains in the three-generation quark mixing matrix, the Cabibbo-Kobayashi-Maskawa (CKM) matrix. The matrix is defined as:

$$V = \begin{bmatrix} V_{ud} & V_{us} & V_{ub} \\ V_{cd} & V_{cs} & V_{cb} \\ V_{td} & V_{ts} & V_{tb} \end{bmatrix}$$

$$= \begin{bmatrix} 1-\frac{1}{2}\lambda^2 & \lambda & A\lambda^3(\rho - i\eta) \\ -\lambda\left[1 + A^2\lambda^4(\rho+i\eta)\right] & 1-\frac{1}{2}\lambda^2 & A\lambda^2 \\ A\lambda^3\left[1-(\rho+i\eta)(1-\frac{1}{2}\lambda^2)\right] & -A\lambda^2\left[(1-\frac{1}{2}\lambda^2)+\lambda^2(\rho+i\eta)\right] & 1 \end{bmatrix}$$

where the latter matrix is the Wolfenstein approximation to order $\lambda^5$. $\lambda$ is the Cabibbo angle and is about 0.22, $A \simeq 1$ and $\rho \neq 0$. The complex elements are $V_{ub}$ and $V_{td}$, if $\eta \neq 0$.

In general, there are three sources of CP violation: CP violation in decay ('direct CP violation'), where the decay amplitude for a process and its' complex conjugate are not the same; CP violation in mixing ('indirect CP violation'), which occurs when two neutral mass eigenstates are not CP eigenstates. CP violation can also originate from interference between direct decays and decays via mixing, if neutral B and $\bar{\text{B}}$ mesons decay into the same final CP eigenstate. All these types of CP violation have been observed in kaon decays, most recent case being the direct CP violation, which the KTeV experiment could observe, thus confirming the earlier results of NA31. Preliminary results from NA48 are in agreement with the KTeV and NA31 measurements (for a review, see Ref. [1] in these proceedings). Kaon decays have provided a wealth of CP violation measurements, but they have not been able to probe the complex elements of the CKM matrix, and thus the SM origin of the CP violation. For this purpose, observing CP violation in B decays is mandatory.

The B mesons are expected to exhibit large CP-violation effects in some (rare) decay modes, which probe the so-called Unitarity Triangle. Unitarity of the CKM matrix defines triangle relations. The one which relates the first and the third column of the CKM matrix turns out to form a triangle in which all the sides are of the same order of magnitude:

$$V_{ud}V_{ub}^* + V_{cd}V_{cb}^* + V_{td}V_{tb}^* = 0.$$

When all the sides are divided by $|V_{cd}V_{cb}^*| \simeq A\lambda^3$ so that the base of the triangle is along the real axis and normalized to 1, the apex of the triangle is located at $(\bar{\rho}, \bar{\eta})$, where $\bar{\rho} = \rho(1 - \lambda^2/2)$ and $\bar{\eta} = \eta(1 - \lambda^2/2)$. One side of the triangle is related to $V_{ub}^*$, $V_{ud}V_{ub}^*/V_{cd}V_{cb}^* \simeq 0.4$, and the other side is related to $V_{td}$, $V_{td}V_{tb}^*/V_{cd}V_{cb}^* \sim 1$. The angles $\alpha$, $\beta$ and $\gamma$ are defined in Fig. 1. Another triangle can be defined by combining the first and the third rows of the CKM matrix, and it is shown in Fig. 2. It probes the same two CKM matrix elements as the 'standard' Unitarity Triangle, and it's angles $\gamma'$ and $\delta\gamma$ can be measured.

When neutral B and $\bar{\mathrm{B}}$ mesons decay into the same final CP eigenstate, the CP violation can in general have contributions both from direct CP violation and from interference between direct and mixed decays. In this case, the time-dependent CP asymmetry can be expressed as follows:

$$a_{CP}(t) = \frac{\Gamma(\mathrm{B_q^0}(t) \to \mathrm{f}) - \Gamma(\bar{\mathrm{B}}_\mathrm{q}^0(t) \to \mathrm{f})}{\Gamma(\mathrm{B_q^0}(t) \to \mathrm{f}) + \Gamma(\bar{\mathrm{B}}_\mathrm{q}^0(t) \to \mathrm{f})}$$

$$= A_{CP}^{dir}(\mathrm{B_q^0} \to \mathrm{f})\cos(\Delta m_q t) + A_{CP}^{int}(\mathrm{B_q^0} \to \mathrm{f})\sin(\Delta m_q t),$$

where $A_{CP}^{dir}$ is the direct CP-violation amplitude and $A_{CP}^{int}$ is the mixing-induced CP-violation amplitude. Subscript q indicates a d- or an s-quark, and $\Delta m_q$ is the mass difference of the $\mathrm{B_q^0}$ eigenstates. Here it is assumed that there is no width difference of the $\mathrm{B_q^0}$ eigenstates, which is valid for $\mathrm{B_d^0}$ mesons. For $\mathrm{B_s^0}$, however, the width difference can be sizeable, 15% or so, and the formula has to be modified accordingly.

If the decay of a neutral B meson is dominated by a single CKM amplitude, the mixing-induced CP-violation amplitude is $A_{CP}^{int} = \Lambda \sin(\phi_M - \phi_D)$. The mixing phase $\phi_M$ is $+2\beta$ in case of $\mathrm{B_d^0}$ mesons and $-2\delta\gamma$ for $\mathrm{B_s^0}$ mesons, and $\Lambda$ is the CP eigenvalue of the final state. The CP-violating weak decay phase $\phi_D$ is zero for dominant $\bar{b} \to \bar{c}cs(d)$ amplitudes, and $-2\gamma$ for dominant $\bar{b} \to \bar{u}ud(s)$ amplitudes.

# 2 Measurement methods

In the past few years, much theoretical progress has been made in understanding the different sources of CP violation, and analysis methods have been developed accordingly. Here, the measurement methods of angles $\beta$, $\alpha$ and $\gamma$ are described, with an emphasis on the proposed new modes. These issues are described in more detail in the theoretical contributions to this conference, see [2], [3] and [4]. Analysis methods are also addressed briefly.

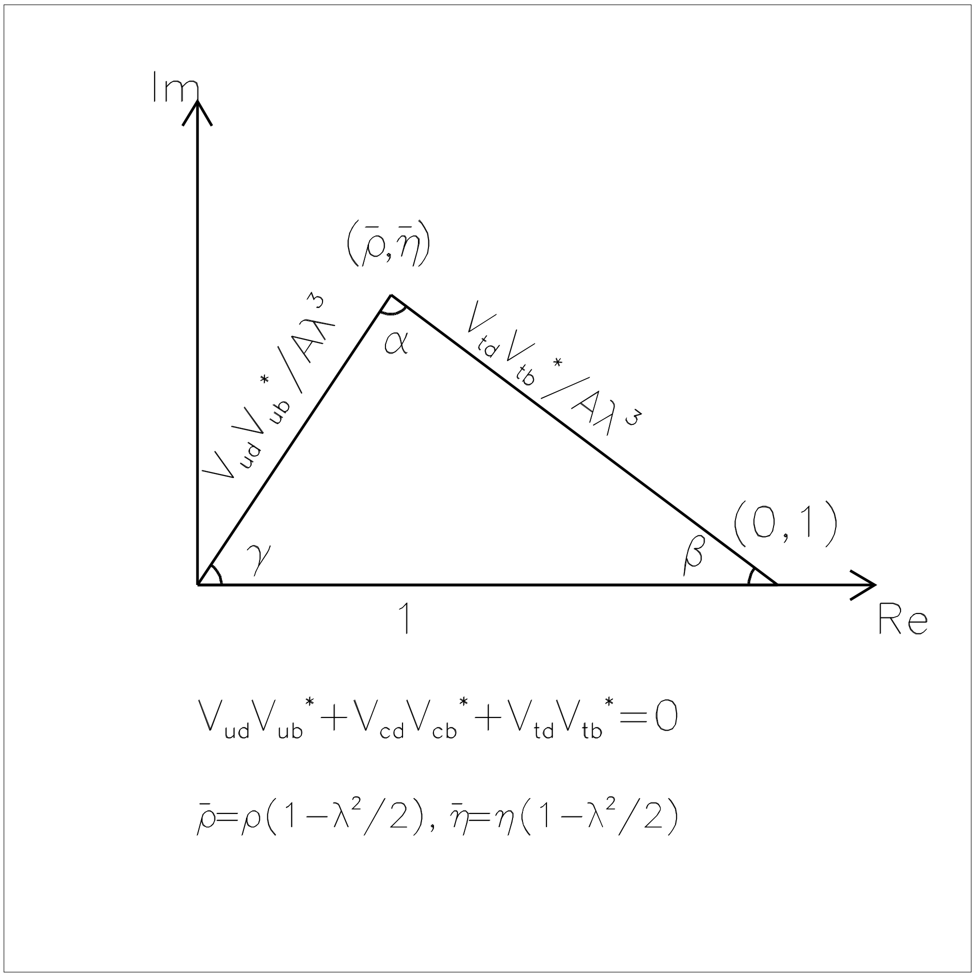


Figure 1: Unitarity triangle $V_{ud}V_{ub}^* + V_{cd}V_{cb}^* + V_{td}V_{tb}^* = 0$.

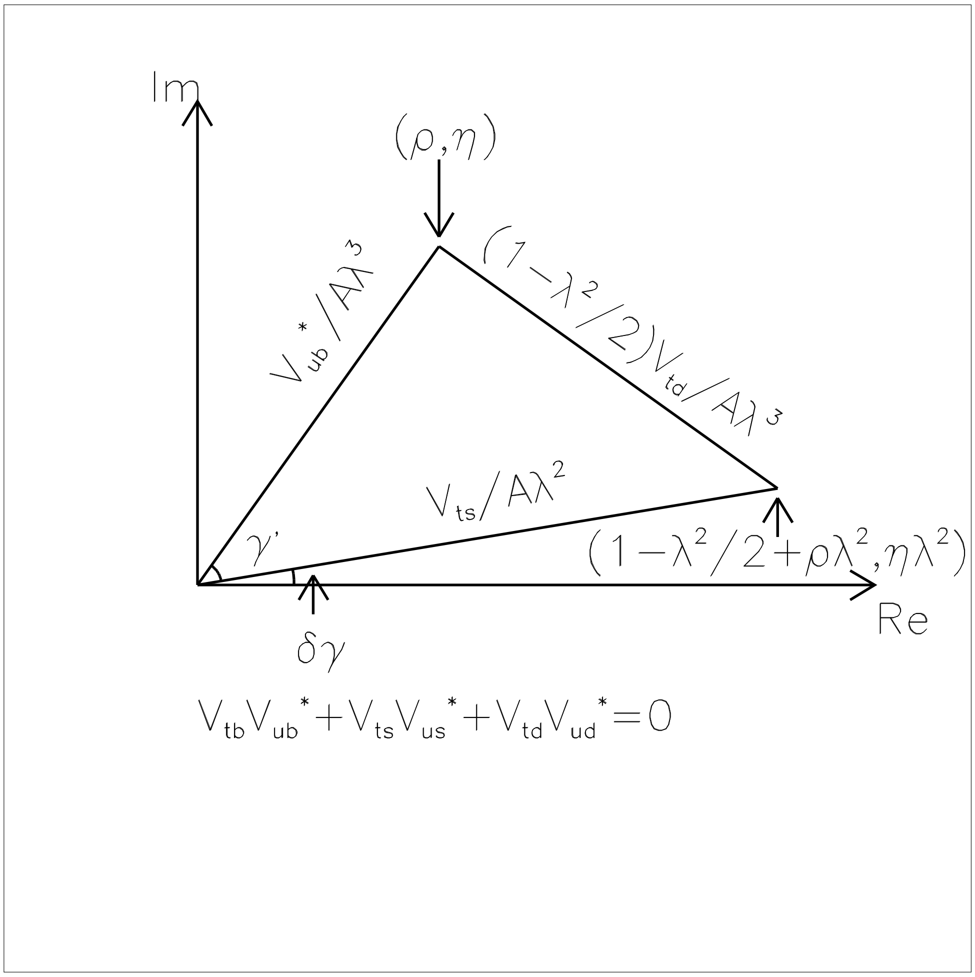


Figure 2: Unitarity triangle $V_{tb}V_{ub}^* + V_{ts}V_{us}^* + V_{td}V_{ud}^* = 0$.

## 2.1 Angle $\beta$

The angle $\beta$ can be measured cleanly using the decays $\mathrm{B_d^0} \to \mathrm{J}/\psi \mathrm{K_S^0}$. This decay is dominated by the decay amplitude $\bar{b} \to \bar{c}cs$, since the penguins are expected to be small and moreover, they have the same weak phase as the tree-level decays. Therefore, the direct CP-violation contribution is very small and can be neglected, *i.e.* $A_{CP}^{dir} \simeq 0$, and the mixing-induced CP-violation amplitude is $A_{CP}^{int} = -\sin 2\beta$.

## 2.2 Angle $\alpha$

The angle $\alpha$ can be measured with the decay $\mathrm{B_d^0} \to \pi^+\pi^-$. This decay has, however, contributions from both penguin and tree decay graphs, and recent CLEO measurements of $\mathrm{B} \to \pi\pi, \mathrm{K}\pi$ indicate that the penguins play a significant role. If there were no penguin contributions present, the mixing-induced CP-violation amplitude would be $A_{CP}^{int} = \sin(2\beta + 2\gamma) = -\sin 2\alpha$, assuming the SM triangle relation $\alpha + \beta + \gamma = \pi$. Including the penguin contributions the amplitudes can be written in the form:

$$A_{CP}^{dir} = 2\frac{A_P}{A_T}\sin\delta\sin\alpha,$$

$$A_{CP}^{int} = -\sin 2\alpha - 2\frac{A_P}{A_T}\cos\delta\cos 2\alpha\sin\alpha,$$

where $A_P/A_T$ is the ratio of the penguin and tree amplitudes, and $\delta$ is the strong phase difference between the amplitudes. If the ratio $A_P/A_T$ can be predicted accurately with the help of additional branching ratio measurements, $\alpha$ and $\delta$ can be extracted from the measured asymmetry.

There is an alternative proposal of measuring the angle $\alpha$ using decays $\mathrm{B_d^0} \to \rho\pi$ [5]. This option has been studied recently for example by the BaBar collaboration [6]. Another way of attacking the problem is to use isospin relations between the decays $\mathrm{B_d^0} \to \pi^+\pi^-$, $\mathrm{B_d^0} \to \pi^0\pi^0$, $\mathrm{B^+} \to \pi^+\pi^0$ and the charge conjugated modes [7]. In this way the angle $\alpha$ could be measured unambiguously. The decay mode $\mathrm{B_d^0} \to \pi^0\pi^0$ is, however, predicted to have a branching ratio of $10^{-6}$ or less, which makes the method experimentally difficult.

## 2.3 Angle $\gamma$

The angle $\gamma$ is the most difficult to measure, since there is no both experimentally feasible and theoretically clean decay of a B to a CP eigenstate, which could be used (the equivalent channel to $\mathrm{B_d^0} \to \mathrm{J}/\psi\mathrm{K_S^0}$ and $\mathrm{B_d^0} \to \pi^+\pi^-$ would be $\mathrm{B_s^0} \to \rho\mathrm{K_S^0}$). There has been, however, a considerable amount of theoretical activity recently to find new methods of probing the angle $\gamma$.

A method of measuring the angle $\gamma$ is to measure the decay time distributions of $B_s^0 \to D_s^{\pm} K^{\mp}$ and the charge conjugated modes [8]. Here CP violation is due to interference of direct and mixed decays. Tagging is obviously needed to distinguish $B_s^0$ and $\bar{B}_s^0$. Fitting the two decay asymmetries *vs.* decay time gives $\gamma - 2\delta\gamma$ and $\delta$, where $\delta$ is the strong phase, and $\delta\gamma$ is the phase of $V_{ts}$.

Another method of measuring the angle $\gamma$ is to consider the decays $B_d^0 \to D_{CP}^0 K^*$, $B_d^0 \to \bar{D}^0 K^*$, $B_d^0 \to D^0 K^*$ and their charge conjugated modes [9]. The amplitudes of these decays are related by two triangles in the complex plane. The triangles differ in the length of one side only, and an angle between the two triangles is $2\gamma$. In addition to the weak phase, there is a dependence on a strong phase difference $\delta$, but it can be extracted from the measurements. Similar relations exist for the charged B decays: $B^+ \to D_{CP}^0 K^+$, $B^+ \to \bar{D}^0 K^+$, $B_d^0 \to D^0 K^+$ and charge conjugated modes [10]. These decays are self-tagging, so no external tag is required. On the other hand, these decays are purely hadronic, requiring a hadronic first level trigger. Furthermore, some of the decay modes have small branching ratios, which make the measurements difficult, in particular for BaBar and BELLE.

The decay $B_d^0 \to D^{(*)\pm}\pi^{\mp}$has been proposed already a while ago for angle $\gamma$ measurement [11]. Even if these decays are not decays to CP eigenstates, both $B_d^0$ and $\bar{B}_d^0$ can decay to the same final state, leading to interference between mixing and decay, which measures $\sin(2\beta + \gamma)$, and a strong phase difference $\delta$. When the angle $\beta$ will have been measured accurately in the $B_d^0 \to J/\psi K_S^0$ decays, the angle $\gamma$ can be extracted. These decays were first payed little attention due to problems with statistics – even if the branching fractions are not that small, of the order of $10^{-3}$, one of the decay paths is doubly Cabibbo-suppressed and therefore the CP-violating effects are tiny. Furthermore, the reconstruction efficiency is small for fully reconstructed final states. The channel was, however, recently re-considered by BaBar [6], for which the channel would provide an access to the angle $\gamma$ since $B_d^0$ decays are involved. They realized that the statistics can be improved considerably by using inclusive reconstruction. The channel has also been studied by LHCb collaboration with promising results, indicating an accuracy of four degrees for the angle $\gamma$ after five years of data-taking [12].

A lot of theoretical effort has been put recently in learning how to extract angle $\gamma$, or set limits to $\gamma$, using various combinations of $K\pi$, $\pi\pi$, and KK final states. Here these modes are addressed only briefly, more details can be found elsewhere in these proceedings [2], [3], [4]. Three different combinations of these decays have been proposed to set limits to the angle $\gamma$: $B^{\pm} \to \pi^{\pm} K$ and $B_d^0 \to \pi^{\mp} K^{\pm}$ [13], $B^{\pm} \to \pi^{\pm} K$ and $B^{\pm} \to \pi^0 K^{\pm}$ [14], [15], and $B_d^0 \to \pi^0 K$ and $B_d^0 \to \pi^{\mp} K^{\pm}$ [15]. The strategies are based on flavour-symmetry arguments, although the theoretical understanding of the hadronic final state interaction effects is poor at the moment.

The strategies of simultaneously determining $2\beta$ and $\gamma$ using decays $B_d^0 \to \pi^+\pi^-$ and $B_s^0 \to K^+K^-$ was also discussed in this conference [3]; using this combination of decays is theoretically cleaner, since the theoretical accuracy is only limited by U-spin breaking effects (interchanging d and s-quarks). Similar arguments were presented for decays $B^0_{s(d)} \to J/\psi K^0_S$ and $B^0_{d(s)} \to D^+_{d(s)} D^-_{d(s)}$.

## 2.4 Measurements of $B^0_s$-mesons

The $B^0_s$-meson mixing parameter $\Delta m_s$ has not been measured yet, due to the rapid oscillations of $B^0_s$-mesons. The $B^0_s$-meson mixing gives an important constraint to the Unitarity Triangle. One side of the triangle is proportional to $V_{td}$, which is related to the $B^0_d$-meson mixing parameter $\Delta m_d$. Despite of the fact that there is a rather precise measurement of $\Delta m_d$, several hadronic uncertainties limit the precision of the $V_{td}$ measurement. In the ratio $\Delta m_s/\Delta m_d$, on the other hand, many common factors such as QCD corrections and dependence on the top quark mass cancel, and a more accurate estimation of $V_{td}$ is possible. The ratio can be written as

$$\frac{\Delta m_s}{\Delta m_d} = \frac{m(B_s)}{m(B_d)} \frac{B(B_s) f^2(B_s)}{B(B_d) f^2(B_d)} \frac{|V^*_{tb} V_{ts}|}{|V^*_{tb} V_{td}|},$$

where $m(B_q)$ are the B-meson masses, $B(B_q)$ are the bag parameters, and $f(B_q)$ the B-meson form factors. In order to measure the $B^0_s$-mixing, the decay time has to be measured accurately, and the flavour of the B has to be tagged both at the decay time (tagged by the observed decay itself) and at production. To tag the flavour of the B at the production time, an external tag has to be used – these tagging methods are discussed in more detail in the following section. The asymmetry between mixed and non-mixed decays is:

$$A(t) = D \frac{\cos(\Delta m_s t)}{\cosh(\Delta\Gamma_s t/2)},$$

where the dilution factor $D$ comes from finite proper time resolution, mistags, and background. $\Delta\Gamma_s = \Gamma_H - \Gamma_L$ is the width difference between the $B^0_s$ mass eigenstates $B_H$ and $B_L$. Oscillations are most often searched for using methods based on fitting the amplitude of the oscillatory term, keeping the $\Delta m_s$ fixed, and repeating the fit with different values of $\Delta m_s$ [16]. This method has the advantage that results from different experiments can be easily combined.

The decay channel $B^0_s \to J/\psi\phi$ is very useful for extracting various, as yet unmeasured or poorly measured parameters of the $B^0_s$ mesons. Furthermore, the decay channel is experimentally an easy one since it can be triggered and reconstructed cleanly. The $B^0_s$ decay proper time and the angular distributions of the secondary particles can be used for extracting $\Delta\Gamma_s$, $\Gamma_s = (\Gamma_H + \Gamma_L)/2$, and CP amplitudes $A_{||}$ and $A_T$ describing the decays to CP-even and CP-odd configurations. The angular analysis is sensitive to the strong phase differences between the amplitudes as well. All these parameters can measured by using untagged samples.

The weak phase of the decay $B^0_s \to J/\psi\phi$ is proportional to $2\delta\gamma$, and it is very small in the SM. Furthermore, the weak phase measurement requires an external tag. Nevertheless, this decay mode can be used for constraining the angle $\gamma$ together with the various other decay modes. In particular, larger than expected CP violation would indicate that processes beyond the SM are involved.

### 2.5 Analysis methods

Experimental analysis methods have been improved considerably over the years. In particular, many new or complementary tagging methods have been established; in addition to the traditional opposite-side lepton tagging and kaon tagging, hadronic tagging methods such as same-side pion tagging, same- or opposite side jet-charge tagging, and vertex charge tagging have shown their power in increasing the statistics significantly. The CDF experiment, for example, has demonstrated that the poorer purity of the hadronic tags is compensated by the bigger efficiency, and the tagging quality factor $\epsilon D^2$ ($\epsilon$ = efficiency, $D$ = dilution) is roughly the same for the opposite side lepton tags (2.2%) as for the same-side hadron tags (2.1%) and the jet-charge tags (2.2%) [17]. The combined use of these methods has allowed the experiments at LEP, SLC and Tevatron to push the limits of their B-physics programmes by improving considerably the tagging efficiency. Measurements of $\Delta m_d$, limits on the $\mathrm{B_s^0}$-mixing, and the asymmetry measurement of tagged $\mathrm{B_d^0} \to \mathrm{J}/\psi \mathrm{K_S^0}$ decays in particular, are examples of results unforeseen some years ago.

In the early days of planning CP-violation measurements using B-decays, expected performance was evaluated by simply estimating event rates. More thorough analysis methods are needed to extract all the available information. For example, time-dependent measurement of CP-asymmetries is almost mandatory, not only to prove the expected time-dependence of the asymmetry, but also to help in distinguishing the signal from backgrounds with different time-dependence. For mixing measurements, amplitude fits have provided a useful platform at LEP, SLC and Tevatron to extract and combine experimental limits. Angular analyses will have to be utilized for channels in which the B-meson decays into spin-carrying non-stable particles, such as in the case of $\mathrm{B_s^0} \to \mathrm{J}/\psi\phi$ decay.

## 3 Present results

### 3.1 Direct measurement of angle $\beta$

The CDF limit on angle $\beta$ was reported in this conference [17]. The $\mathrm{B_d^0} \to \mathrm{J}/\psi \mathrm{K_S^0}$ sample consisted of about 200 events in which both muons from $\mathrm{J}/\psi$ are within the SVX acceptance, and about 200 events with one or no muons reconstructed in the SVX. Data were collected at the Tevatron Run I, and consisted of an integrated luminosity of 110 $\mathrm{pb}^{-1}$. The events with both muons in the SVX had a precise lifetime information, and a time-dependent analysis could be performed. The additional sample of 200 events had imprecise lifetime information. A time-averaged analysis could be performed, however, improving the precision of the combined measurement. Soft leptons, jet-charge, and same-side hadrons were used for tagging, each providing a similar tagging quality of about 2.2%. The combined tagging quality factor was (6.3±1.7)%, accounting for correlations and double tags. The tagging efficiency and dilution factors were measured using an independent sample of $B^+ \to J/\psi K^+$ decays, and a $B \to \ell D^{(*)} X$ sample suitably scaled to account for momentum differences. The result of the full unbinned maximum likelihood fit was: $\sin 2\beta = 0.79^{+0.41}_{-0.44}$. The measured asymmetry is shown in Fig. 3. Interpreting the measurement as a limit to $\sin 2\beta$, CDF quote $0 < \sin 2\beta < 1$ at 93% CL using the Feldman-Cousins frequentist approach, and at 95% CL using the Bayesian approach.

The OPAL experiment at LEP performed the first exploratory search for CP asymmetry in $B^0_d \to J/\psi K^0_S$ decays, using a sample of 24 reconstructed events, out of which 10 events were estimated to be background [18]. The measurement yielded $\sin 2\beta = 3.2^{+1.8}_{-2.0} \pm 0.5$.

## 3.2 Precision measurements

The CKM matrix element ratios $|V_{ub}/V_{cb}|$ and $|V_{td}/V_{cb}|$ are related to the lengths of the sides of the Unitarity Triangle. In this conference, updated results were presented by CLEO on $|V_{cb}|$ and $|V_{ub}/V_{cb}|$ [19], yielding

$$|V_{cb}| = (38.5 \pm 2.1 \pm 2.2 \pm 1.2) \cdot 10^{-3},$$

$$|V_{ub}| = (3.25 \pm 0.14^{+0.21}_{-0.29} \pm 0.55) \cdot 10^{-3},$$

where the last error is the theoretical uncertainty. The LEP experiments have made progress in measuring these matrix elements in the LEP1 data, with different systematical uncertainties from CLEO. New results on $|V_{cb}|$ were presented in this conference from analyses using exclusively reconstructed final states, see Ref. [20]; the errors of individual experiments are approaching the ones from CLEO. Averaging over the LEP results, including both the inclusive $|V_{cb}|$ determinations from lifetime and branching ratio measurements and the exclusive measurements, yields [21]:

$$|V_{cb}| = (40.2 \pm 1.9) \cdot 10^{-3}.$$

The LEP average for $|V_{ub}|$ reported in this conference was:

$$|V_{ub}| = (4.03^{+0.39}_{-0.46} \pm 0.56) \cdot 10^{-3},$$

where the last error is the theoretical uncertainty. The matrix element $V_{td}$ is at the moment constrained by the $\Delta m_d$ measurements and the $\Delta m_s$ limits. The

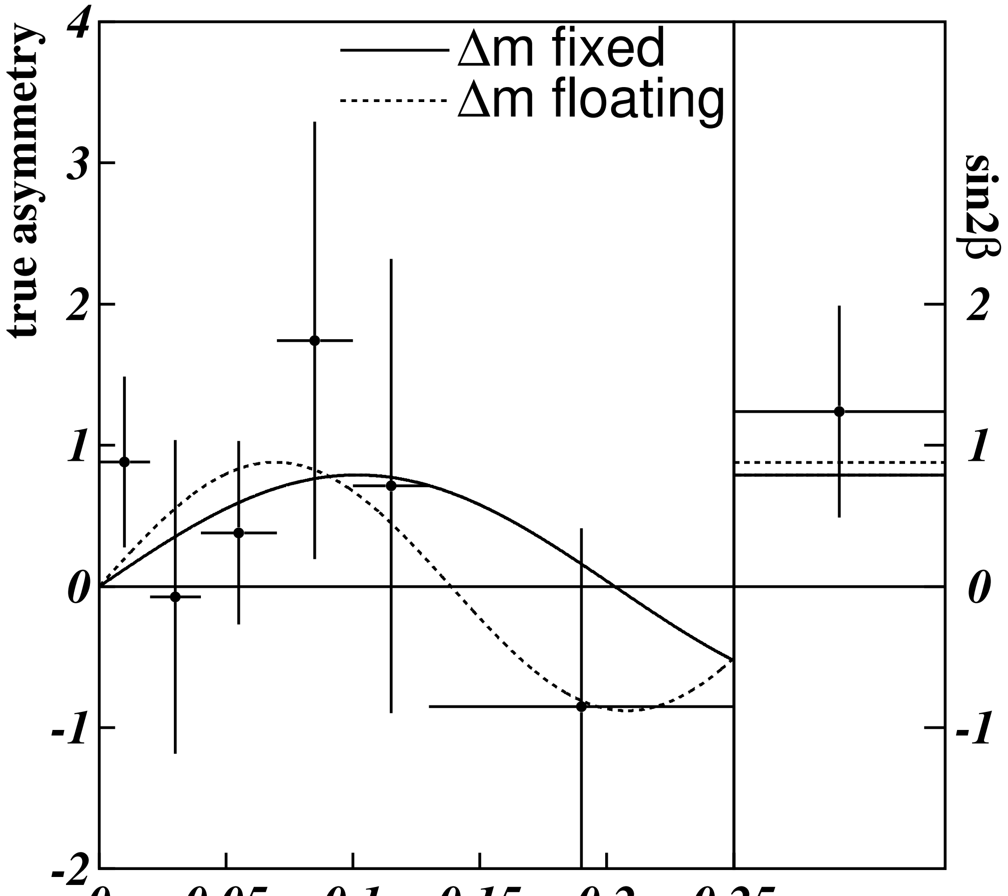


Figure 3: CDF measurement of asymmetry in $B_d^0 \to J/\psi K_S^0$ decays [17].

$\mathrm{B_d^0}$ meson oscillation frequency $\Delta m_d$ has been measured accurately by the LEP experiments, SLD and CDF, while the $\Upsilon(4S)$ experiments provide time-integrated mixing measurements. The LEP average value reported in this conference yields a value of $\Delta m_d = (0.468 \pm 0.019)$ ps$^{-1}$ [20], while the world average including LEP, SLD, CDF and $\Upsilon(4S)$ experiments is $\Delta m_d = (0.473 \pm 0.016)$ ps$^{-1}$ [22]. The combined LEP 95% CL limit for the $\mathrm{B_s^0}$ meson oscillation frequency $\Delta m_s$ is 9.6 ps$^{-1}$, while the sensitivity is 12.6 ps$^{-1}$. The world average limit by the LEP experiments, SLD, and CDF is 14.3 ps$^{-1}$, and the sensitivity is at 14.7 ps$^{-1}$ [22].

Lifetimes of $\mathrm{B^+}$, $\mathrm{B_d^0}$, $\mathrm{B_s^0}$, $\mathrm{B_c}$ and B-baryons were reported by CDF and the LEP experiments. The combined results were [17], [20]:

$$\tau(\mathrm{B^+}) = (1.66 \pm 0.03)\ \mathrm{ps},$$

$$\tau(\mathrm{B_d^0}) = (1.55 \pm 0.03)\ \mathrm{ps},$$

$$\tau(\mathrm{B_s^0}) = (1.47 \pm 0.06)\ \mathrm{ps},$$

$$\tau(\mathrm{B_c}) = (0.46 \pm 0.17)\ \mathrm{ps\ (CDF)},$$

$$\tau(\Lambda_\mathrm{b}) = (1.23 \pm 0.08)\ \mathrm{ps},$$

$$\tau(\Xi_\mathrm{b}^0) = (1.39^{+0.34}_{-0.28})\ \mathrm{ps\ (ALEPH,\ DELPHI)}.$$

Very recently, new branching ratio measurements were presented by CLEO [23]. The measured branching ratio for the decay $\mathrm{B_d^0} \to \pi^+\pi^-$, $\mathrm{BR}(\mathrm{B_d^0} \to \pi^+\pi^-) = (4.7^{+1.8}_{-1.5} \pm 1.3) \cdot 10^{-6}$, indicates difficulties for the angle $\alpha$ measurements, in particular at the $\mathrm{e^+e^-}$ B-factories. The much larger branching ratio for the decay $\mathrm{B_d^0} \to \mathrm{K}^-\pi^+$, $\mathrm{BR}(\mathrm{B_d^0} \to \mathrm{K}^-\pi^+) = (1.88^{+0.28}_{-0.26} \pm 0.06) \cdot 10^{-5}$, suggests large penguin contributions. CLEO is also probing the way of constraining the angle $\gamma$ by comparing the rates for charged and neutral B decays to $\mathrm{K}\pi$ using the Neubert-Rosner analysis. CLEO results [19] favour $\gamma > 90°$, a result which would be in contradiction with the Unitarity Triangle apex region allowed by the $\Delta m_s$ limit.

CDF presented complementary results on the $\mathrm{B_s^0}$ frontier [17]. Using a sample of about 600 inclusively reconstructed $\mathrm{B_s^0} \to \ell \mathrm{D_s} \mathrm{X}$ decays, a two-component lifetime fit of the form $\exp(-\Gamma_H t) + \exp(-\Gamma_L t)$ was used to measure the width difference $\Delta\Gamma_s$, yielding a result $\Delta\Gamma_s/\Gamma_s = 0.34^{+0.31}_{-0.34}$. Interpreted as a limit, the measurement yielded $\Delta\Gamma_s/\Gamma_s < 0.83$ at 95% CL. In the SM, the width difference $\Delta\Gamma_s$ is related to $\Delta m_s$ by a hadronic scale factor. The CDF limit on upper limit on $\Delta\Gamma_s$ gives thus an upper limit of 96 ps$^{-1}$ to $\Delta m_s$.

CDF presented also polarisation measurements. The measurement of the polarisation in $\mathrm{B_d^0} \to \mathrm{J}/\psi \mathrm{K}^{*0}$ used about 200 events, similar to CLEO. The polarisation measurement of $\mathrm{B_s^0} \to \mathrm{J}/\psi\phi$ used about 40 events – it is the first polarisation measurement of its kind, albeit limited by the statistics. With a larger statistics, $\Delta\Gamma_s$ can be measured together with the CP-even and CP-odd amplitudes $A_{||}$ and $A_T$, along with the strong phases, as discussed in Section 2.4.

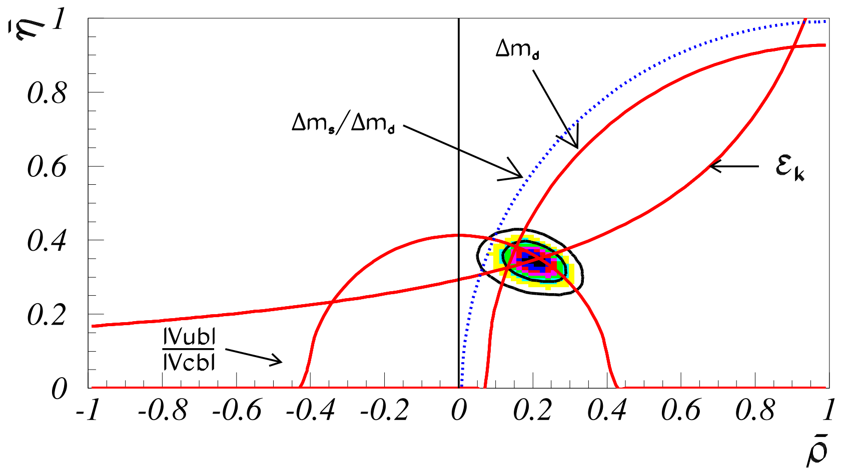


Figure 4: Unitarity Triangle constraints from present precision data (from Ref. [24]).

The precision data on $|V_{cb}|$, $|V_{ub}/V_{cb}|$ and $\Delta m_d$, the $\Delta m_s$ limit, and $\epsilon_K$ from kaon experiments, combined with estimates on hadronic factors from mass measurements and lattice calculations, can be used to constrain the Unitarity Triangle. Various such fits have been performed, see for example Refs. [24], [25] and [26]. Theoretical errors for the $V_{ub}$ are already limiting the bound from $|V_{ub}/V_{cb}|$. The direct measurement of angle $\beta$ is completely consistent with the region allowed by the indirect measurements, but the present accuracy of the $\sin 2\beta$ measurement does not improve the overall fit. In Ref. [24], the following ranges for the angles $\alpha$, $\beta$ and $\gamma$ are quoted:

$$\sin 2\beta = 0.725^{+0.050}_{-0.060},$$

$$\sin 2\alpha = -0.26^{+0.29}_{-0.28},$$

$$\gamma = (59.5^{+8.5}_{-7.5})^{\circ}.$$

The region limited in the complex space by the combined fit is shown in Fig. 4.

# 4 Experiments embarking on data taking

The timing of the conference was quite exciting, since there were several B-experiments getting ready for data-taking. This conference was the first one to see collision events from BaBar and BELLE. HERA-B experiment is expected to be fully commissioned by end of 1999, and the upgraded CDF and D0 experiments will re-start at the high-luminosity Tevatron around mid-2000.

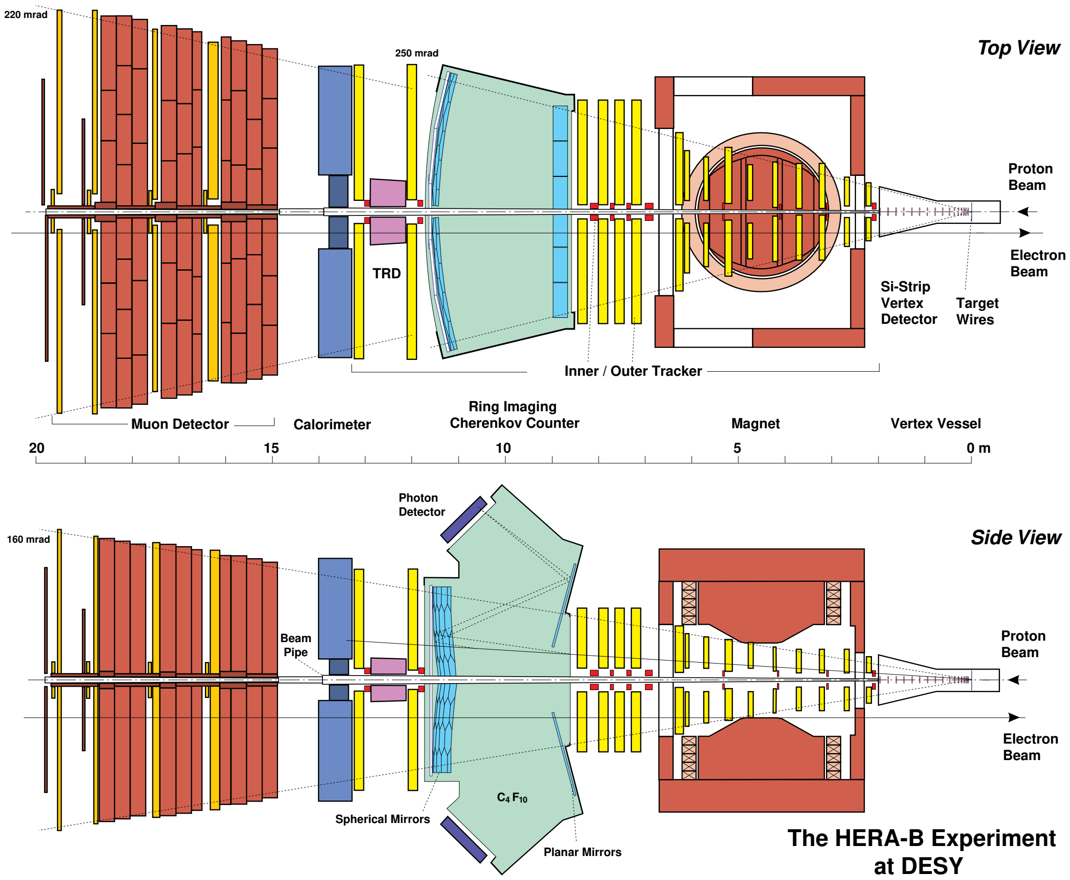


Figure 5: The HERA-B detector layout.

## 4.1 HERA-B

HERA-B experiment at DESY is a fixed-target B-experiment, operating at the 920 GeV proton ring HERA [27]. The detector layout is shown in Fig. 5. The experiment is challenging due to the small ratio of $b\bar{b}$-to-total cross-section, about $10^{-6}$, resulting in difficult trigger and target requirements. At the center-of-mass energy of about 40 GeV, the $b\bar{b}$ cross-section is about 12 nb, albeit with large uncertainties. In order to obtain a competitive number of signal events in the decay mode $B_d^0 \to J/\psi K_S^0$ (1500 reconstructed events in a year), four interactions per bunch crossing are needed, resulting in an interaction rate of 40 MHz. This corresponds to an integrated luminosity of about 30 $fb^{-1}$ in a year. The requirements to the trigger, and the high radiation dose that some of the HERA-B subdetectors will have to stand, are comparable to the conditions at LHC.

To maximise the interaction rate while minimising the interference to the ep-operation at HERA, the target was designed to consist of two sets of four wires placed at the beam halo, located at a distance of four to ten standard deviations from the beam [28]. The target has been in continuous operation since 1997, and the main requirements have been achieved.

The HERA-B trigger consists of three levels [29]. The first level trigger searches for two lepton candidates with an invariant mass compatible with a $J/\psi$, or two high-$p_T$ hadrons compatible with originating from a B-meson. The track seeds originate from the muon pad chambers, the electromagnetic calorimeter or from the high-$p_T$ chambers. A fast hardware tracking is then performed, in which regions of interest are scanned in the upstream detector layers using a Kalman filter-type method. The track candidates are refined in the second level, while the third level trigger uses data outside regions of interest as well. The final output level (level 4) reconstructs and classifies the events without any further rate reduction.

Many of the sub-detectors are completed and entering the full commissioning phase: the vertex detector (VDS) [30], the Ring Imaging Cherenkov Counter (RICH) [31], electromagnetic calorimeter (ECAL) [32], the TDR and the muon detector [33]. The data-acquisition system has been running stable for several months, and the commissioning of the first level trigger (FLT) is starting. Some HERA-B subdetectors have been suffering from technological problems to fulfil the requirements of operating in a high-radiation environment. The anode aging and Malter effect problems with the outer tracker, which consists of honeycomb drift-chambers, seem to have been solved by cathode Au-coating, proper gas choice and careful validation of materials as well as manufacturing procedures. After applying these measures, the detectors have been proven to survive in a hadronic environment an equivalent radiation dose of two integrated HERA-B years [34]. The mass production is progressing in a rapid pace, and all the chambers are planned to be installed by November 1999. The inner tracker is using MicroStrip Gas Chambers (MSGCs). Original problems with sparking were solved by adding Gas Electron Multipliers (GEMs) into the drift space. Even though the chambers still show a gain variation as a function of the accumulated charge, the detectors have been considered as adequate for HERA-B [35]. The mass production is proceeding and the whole inner tracker is expected to be completed by the end of 1999.

## 4.2 $e^+e^-$ B-factory experiments

The BaBar experiment at SLAC and the BELLE experiment at KEK are asymmetric $e^+e^-$ collider experiments, collecting $B\bar{B}$ pairs produced in $\Upsilon(4S)$ decays. The production cross-section of $b\bar{b}$ pairs is about 1 nb. Both experiments took their first data just prior to this conference, and exciting first event views were shown.

In BaBar, the 9 GeV electron and 3.1 GeV positron beams, circulating in the double PEPII ring, are brought to collide with a zero-angle crossing, which requires strong magnets within the interaction region to deflect the beams between bunches. The nominal luminosity is $3 \cdot 10^{33}$ cm$^{-2}$s$^{-1}$ – the nominal one year data corresponds thus to 30 $\mathrm{fb}^{-1}$. The BaBar detector has to fulfil special requirements on its' tracking parts due to the asymmetric collisions: since the boost is along the beam axis, the difference of the decay times of the two B-mesons is measured by the difference in the $z$ component of the vertex separation. Furthermore, the $p_{\mathrm{T}}$-range of the final state particles is quite low, between 60 MeV and 4 GeV. The tracking system consists of a Silicon Vertex Tracker (SVT) and a drift chamber (DCH), immersed in a 1.5 T solenoidal field. The charged hadrons are identified in the Detector for Internally Reflected Cherenkov light (DIRC), which is a novel technology using quartz bars both for producing the Cherenkov light and as light guides [36]. The electromagnetic calorimeter is a CsI calorimeter, and outside the EMC the Instrumented Flux Return (IFR) is used for muon identification and for enhancing $\mathrm{K}^0_{\mathrm{L}}$ detection. The collaboration is using software written entirely in C++.

BaBar started taking colliding beam data May 26$^{\mathrm{th}}$ 1999 [37]. By June 17$^{\mathrm{th}}$ 1999, time of the conference, 10 $\mathrm{pb}^{-1}$ were collected on tape and first hadronic events were shown. An example of a reconstructed hadronic event is shown in Fig. 6. Mass peaks for $\mathrm{K}^0_{\mathrm{S}} \to \pi^+\pi^-$ with a width of 6 MeV (loose vertex pointing requirements, no particle ID) and $\pi^0 \to \gamma\gamma$ were reconstructed and shown. In addition, $60 \cdot 10^6$ cosmics had been collected prior to the colliding beam data taking. All subsystems were operational and complete apart from a fraction of the DIRC bars. Since the conference, the exclusive B reconstruction was under way and the first $\mathrm{B}^0_{\mathrm{d}} \to \mathrm{J}/\psi\mathrm{K}^0_{\mathrm{S}}$ candidates were identified.

The BELLE experiment is operating at the KEKB ring, which produces collisions between 8 GeV electron and 3.5 GeV positron beams. The ring design includes several novel features, such as a finite-angle beam crossing, which has the advantage that there is no need for strong magnets within the interaction region, making the design of the tracker detectors easier. The nominal design luminosity is $1 \cdot 10^{34}$ $\mathrm{cm}^{-2}\mathrm{s}^{-1}$. If bunch-bunch instabilities appear, a crab-crossing scheme, in which the bunches are tilted so that they collide head-on despite of the finite crossing angle, will be a possible solution. The tracking system consists of a Silicon Vertex Detector (SVD) and a central drift chamber (CDC) in a 1.5 T solenoidal field. The charged hadrons are identified by using a time-of-flight (TOF) counter and an aerogel Cherenkov counter (ACC). The electromagnetic calorimeter consists of CsI crystals and the instrumented iron yoke serves as a muon and $\mathrm{K}^0_{\mathrm{L}}$ detector.

The first collision events were observed in June 1$^{\mathrm{st}}$ 1999 [38]. By June 10$^{\mathrm{th}}$ 1999, an integrated luminosity of about 530 $\mathrm{nb}^{-1}$ was collected. In this conference, reconstructed $\mathrm{J}/\psi \to \mathrm{e}^+\mathrm{e}^-$ and $\mu\mu$ events were shown, as well as mass peaks for $\mathrm{K}^0_{\mathrm{S}} \to \pi^+\pi^-$ and for $\pi^0 \to \gamma\gamma$. The $\mathrm{K}^0_{\mathrm{S}}$ mass resolution was 2.5 MeV. The resolution for the $\pi^0$ was about 5.6 MeV, with $E_\gamma > 20$ MeV. An example of a reconstructed hadronic event is shown in Fig. 7. After the conference, till August 4$^{\mathrm{th}}$ 1999, a total of 25 $\mathrm{pb}^{-1}$ of data was recorded by BELLE, with the accelerator reaching a peak luminosity of $2.9 \cdot 10^{32}$ $\mathrm{cm}^{-2}\mathrm{s}^{-1}$. Most of the data were taken on

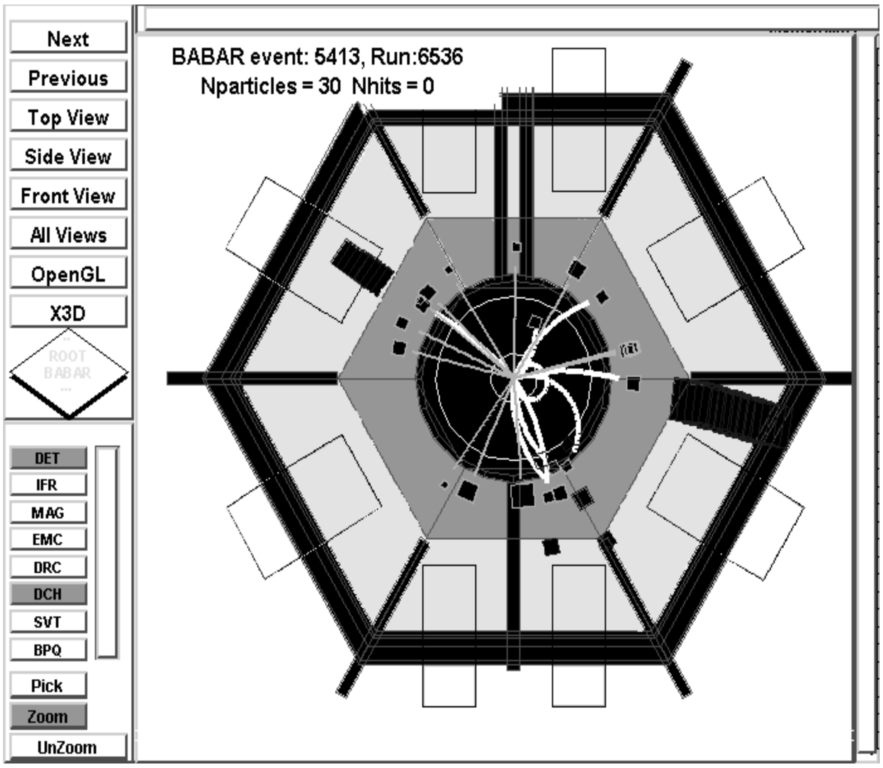


Figure 6: A hadronic event reconstructed in BaBar.

the $\Upsilon(4S)$ peak.

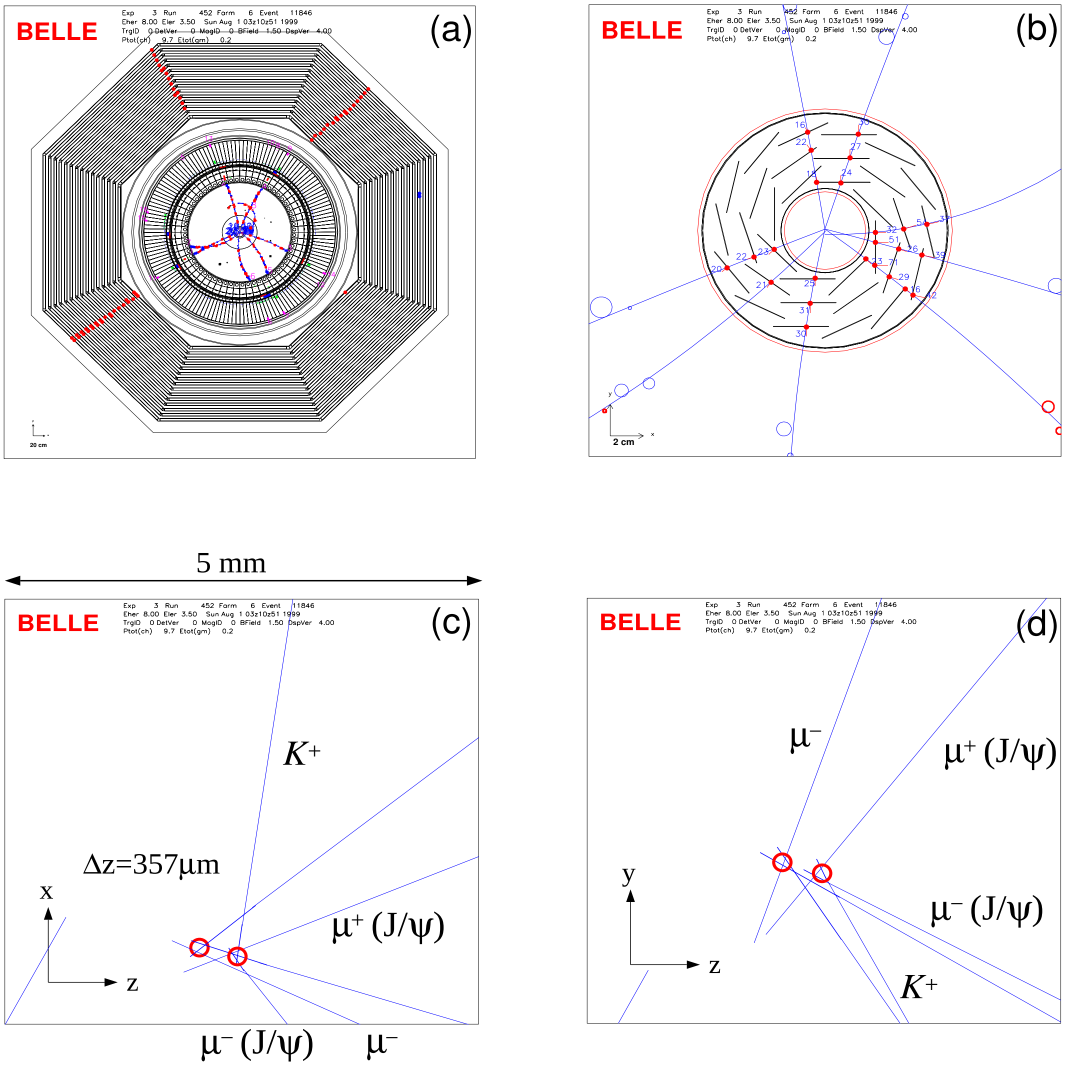


Figure 7: A hadronic event reconstructed in BELLE.

The CLEOIII detector is an upgrade of the CLEO detector at CESR to achieve luminosities in excess of $10^{33}$ cm$^{-2}$s$^{-1}$ [39]. CESR is a symmetric $e^+e^-$ collider operating at the $\Upsilon(4S)$ peak. The main features of the upgrade concerns the particle identification and tracking [40]. Charged hadron identification will be enhanced with a RICH detector. The tracking system had to be rebuilt due to the reduced space available – the new tracker will consists of a new drift chamber, and a silicon vertex detector, whose main function is in providing precision tracking. The CLEOIII experiment will start operating during 1999, and it is aiming at a wide range of B-physics accessible with rate measurements.

## 4.3 Upgraded CDF and D0

The CDF and D0 experiments at the Tevatron $p\bar{p}$ collider are being upgraded for the high-luminosity run (RunII). The RunII is scheduled to begin in the summer of 2000, with an increased luminosity resulting from many improvements in the collider, the main one being the replacement of the old Main Ring with the new Main Injector. The crossing rate will be 132 ns for 121 bunches, corresponding to a typical luminosity of $1.62 \cdot 10^{32}$ cm$^{-2}$ s$^{-1}$ and a peak luminosity of $2 \cdot 10^{32}$ cm$^{-2}$ s$^{-1}$. At the peak luminosity, the average number of interactions per crossing is two. The design goal is to collect an integrated luminosity of 2 fb$^{-1}$ in about two years of running. An increase of the collision energy from 1.8 TeV to 2.0 TeV is planned as well, driven by the 40% enhancement in the $t\bar{t}$ yield. At Tevatron, the $b\bar{b}$ production cross-section is about 100 $\mu$b. The ratio of the $b\bar{b}$-to-total cross-section is about $10^{-3}$, requiring efficient trigger strategies.

The CDF detector will have many new features to improve the resolution and radiation tolerance, and to cope with the shorter crossing rate [41]. There will be a new seven-layer radiation hard silicon vertex and tracking system, extending between radii 2.4 cm to 28 cm (1.6 cm with the innermost Layer00, beyond the baseline detector). The central outer tracker, COT, will be new as well, since the available radial space will be less, and the maximum drift time has to be shorter than the crossing time. The calorimeters beyond $|\eta| > 1$ will be replaced with a scintillating tile calorimeter, and a new muon system will be built to cover the region $1.0 < |\eta| < 1.5$. The trigger and data acquisition system will be fully pipelined. Fast tracking will be available at level-1, allowing for an all-hadronic B-decay trigger. In the level-2, it will be possible to trigger on tracks with a high impact-parameter. Beyond the baseline design, a TOF detector has been recommended to enhance particle identification at very low momenta (0.3 GeV $< p_{\mathrm{T}} <$1.6 GeV).

The D0 detector is undergoing a major upgrade, driven by both new physics goals and changes in the collider [42]. The whole tracking system is new, consisting of a Central Fiber Tracker (CFT) and a Silicon Microstrip Tracker (SMT) in a 2 T solenoidal field. The electron identification is enhanced by adding preshower detectors in front of the electromagnetic calorimeter, and the muon system has been upgraded significantly. To cope with the shorter bunch spacing while covering the physics goals, the front-end electronics, trigger and data-acquisition systems have been largely re-designed. The level-1 B-decay triggers are based on soft leptons – hadron or vertex triggers are not considered. In addition to the single and di-muon triggers, $e^+e^-$ pairs can be triggered on by matching either a track element in the outermost CFT layers ($p_{\mathrm{T}}$ threshold 1.5 GeV) and a calorimeter cluster ($E_{\mathrm{T}}$ threshold 1.5 GeV), or a preshower cluster (threshold 2-5 MIPs) and a calorimeter cluster.

# 5 Experiments being designed and constructed

By the year 2005, various experiments will have explored the Unitarity Triangle. It is likely that the angle $\beta$ will have been measured with a fair precision, $\sigma(\sin 2\beta)$=0.05 or so. Sides of the Unitarity Triangle will have been measured: $V_{ub}$, possibly still limited by hadronic uncertainties, and $V_{td}$ from mixing measurements of both $B_d$ and $B_s$. It is still quite possible that for the angle $\alpha$, there is only a low statistics measurement, with theoretical uncertainties, and for the angle $\gamma$, there is no accurate measurement or even no direct measurement at all. Considering the allowed region for the apex of the Unitarity Triangle, the angle $\beta$ is actually not constraining it significantly, but it is the angle $\gamma$ which is significantly reducing the size of the allowed region and thus placing a stringent test to the SM. Therefore, the next generation of experiments at LHC and at Tevatron are needed for full investigation of CP violation in order to over-constrain the CKM matrix via high statistics measurements, complemented by theoretically clean channels.

## 5.1 Dedicated B-physics experiments LHCb and BTeV

LHCb is a forward single-arm spectrometer at LHC with efficient trigger, good particle identification and good momentum resolution [12], [43]. The LHCb detector layout is shown in Fig. 8. The main components of the detector are a vertex detector inside the beam vacuum, a tracking system with a dipole magnet, two RICH counters to identify charged hadrons over a sufficiently large momentum range, calorimeters, and a muon system. The angular coverage is from 15 mrad to 300 mrad, corresponding to about three units in pseudo-rapidity. The single-arm geometry exploits the fact that the $b\bar{b}$ system is boosted along the beam, and thus the B and the $\bar{B}$ mesons are highly correlated in pseudo-rapidity.

At LHC, the total $b\bar{b}$ cross-section is about 500 $\mu$b, with an uncertainty of a factor of two or more. The fraction of $b\bar{b}$-to-total cross-section is of order $10^{-2}$. At LHCb, the LHC beam is 'detuned' to produce a constant luminosity of $2 \cdot 10^{32}$ cm$^{-2}$s$^{-1}$. This luminosity is chosen to optimize the fraction of single pp interactions per bunch crossing to minimize the radiation damage, and to minimize the detector occupancy to make pattern recognition easier. At the luminosity of $2 \cdot 10^{32}$ cm$^{-2}$s$^{-1}$, the fraction of bunches with a single pp interaction is about 30%.

At LHCb, the level-0 trigger selects first single pp interactions by applying a pile-up veto, obtained from two dedicated Si-disks. Single interactions are then passed on to be processed by $p_T$ or $E_T$ single track triggers, provided by muon chambers for muons (20% of events), ECAL for electrons/photons (10%), or ECAL and HCAL for hadrons (60%). The rate is reduced from 40 MHz to 1 MHz.

The level-1 trigger is based on topological identification of secondary vertices.

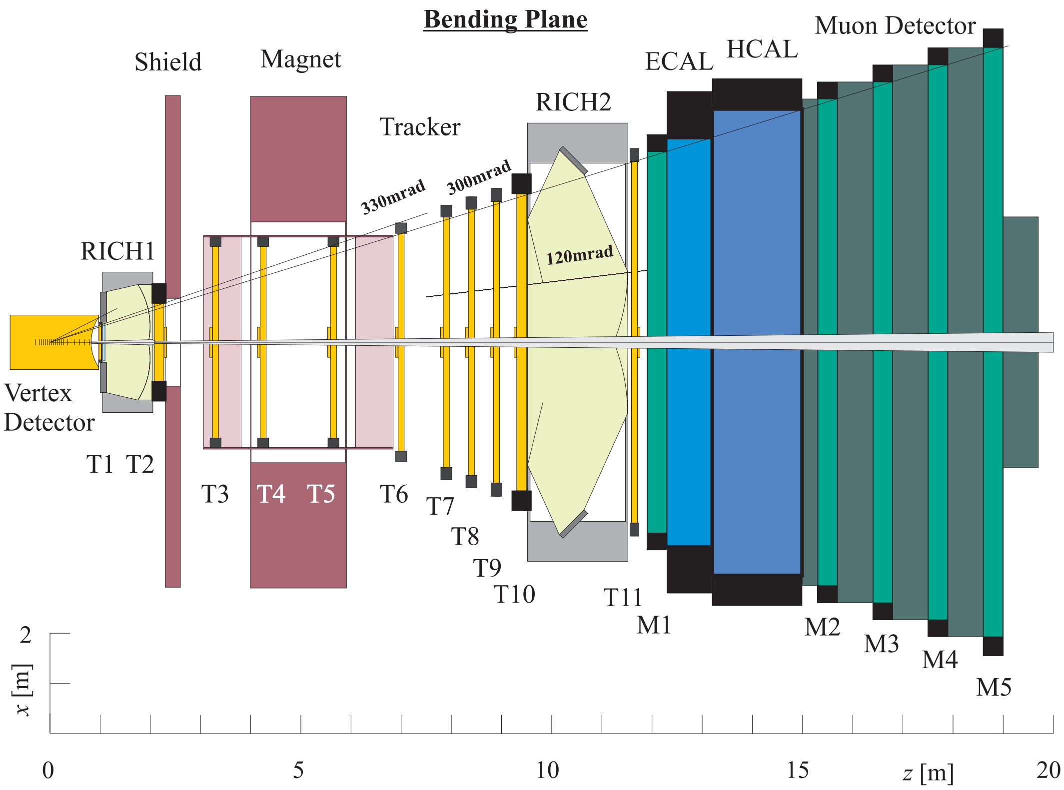


Figure 8: The LHCb detector layout.

Track elements are found in the Si-disks, the primary vertex is reconstructed, and secondary vertices are formed by using large impact parameter tracks. The rate is expected to be reduced from 1 MHz to 40 kHz. The higher level triggers (levels two and three) will consist of software algorithms running on farms of commercial computers. The higher level triggers will have to reject uninteresting $\mathrm{b\bar{b}}$ events in addition to non-b events. The target rate for data recording is 200 Hz.

BTeV is a forward two-arm spectrometer proposed for Tevatron [44], [45]. The BTeV detector layout is shown in Fig. 9. The detector is planned to have a good particle identification, and in particular, it is relying on a secondary vertex level-1 trigger by using track vectors from pixel triplets. The main components of the detector are a pixel vertex detector located inside a dipole magnet on the interaction region, forward trackers, RICH counters, high-resolution $\mathrm{PbWO_4}$ electromagnetic calorimeters, hadron absorbers and muon system consisting of toroid spectrometers. The angular coverage is up to 300 mrad on both arms. The total $\mathrm{b\bar{b}}$ cross-section is a factor of five less than at LHC; however, there are many compensating factors working in favour of BTeV. The two-arm solutions brings an obvious factor of two. Another factor of two comes from running with two interactions per crossing, which is possible at Tevatron due to the long luminous region which makes it easier to separate different primary vertices, and the longer bunch spacing (132 ns). Furthermore, the smaller boost of B hadrons increases the track angles with respect to the beam pipe, thus reducing the radiation damage and making the pattern recognition easier. The smaller boost also enables BTeV to manage with a single RICH detector, whereas LHCb has to use two separate RICHes to cover the whole dynamical range. The overall length of the detector can be made shorter as well.

A vertex trigger at the level-1 is naturally very desirable to trigger efficiently on purely hadronic final states. To achieve this, the tracking/vertex detector design has to be tied closely to the trigger design. The baseline is to use pixel triplets in a dipole field, thus forming track vectors. Primary vertex can be formed from these track vectors, and large impact parameter tracks can be searched for. Preliminary studies indicate that requiring at least two tracks detached by more the four standard deviations from the primary vertex, only 1% of the beam crossings are triggered, while an efficiency from 40% to 70% can be achieved for the most commonly studied hadronic decays ($\mathrm{B^0 \to h^+h^-}$, $\mathrm{B_s^0 \to D_sK}$, $\mathrm{B^- \to D^0K^-}$, $\mathrm{B^- \to K_S^0\pi^-}$, $\mathrm{B_d^0 \to J/\psi K_S^0}$, $\mathrm{B_d^0 \to J/\psi K^*}$, $\mathrm{B^0 \to K^*\gamma}$ ) [45].

## 5.2 General purpose experiments ATLAS and CMS at LHC

The general purpose experiments ATLAS and CMS at LHC are high-$p_\mathrm{T}$ central collider experiments, designed primarily for heavy particle searches, but with

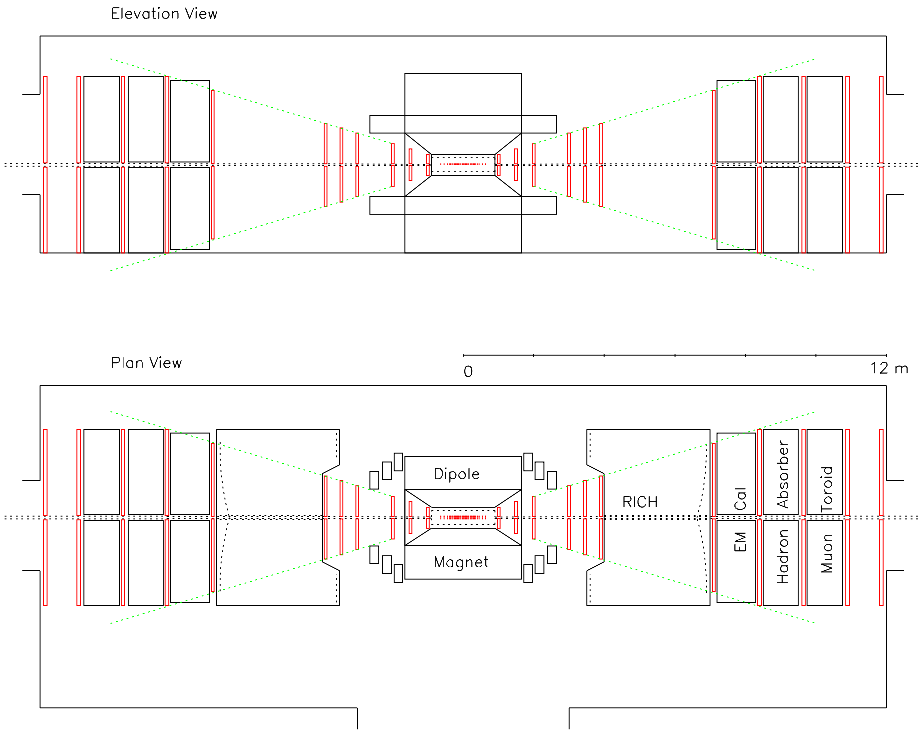


Figure 9: The BTeV detector layout.

a significant capacity for precision physics, in particular in the first years of LHC operation with a nominal 'low' luminosity of $1 \cdot 10^{33}$ cm$^{-2}$s$^{-1}$, giving an integrated luminosity of 10 fb$^{-1}$ per year [46], [47], [48]. The limiting factor for the maximum luminosity for B physics is the level-1 trigger output rate, rather than the offline reconstruction capability. Some channels such as rare decays of the type $\mathrm{B} \to \mu\mu(\mathrm{X})$ are particularly suitable for ATLAS and CMS since they are self-triggering, and the high-luminosity data of LHC can be used as well.

The angular coverage of the tracking systems of these detectors is about five units in pseudo-rapidity. Since the $\mathrm{b\bar{b}}$ production cross-section is roughly flat in pseudo-rapidity, the production rate is as high in the central as in the forward region. On the other hand, the small boost of central b quarks, and the consequent lack of angular correlation between the b and $\mathrm{\bar{b}}$, make triggering of B-hadron final states difficult. The lack of single hadron triggers with sufficiently low $p_{\mathrm{T}}$ at the lowest trigger level, and the poor charged hadron identification are the most obvious handicaps of the general purpose experiments with respect to dedicated B-physics experiments.

Both ATLAS and CMS have powerful muon systems which are capable of triggering on single low-$p_{\mathrm{T}}$ muons at the lowest trigger level – the threshold for a single muon trigger is 6 GeV for ATLAS and 7 GeV for CMS. The single muon trigger makes the backbone of the B-physics triggers. CMS can use a lower threshold of 2-4 GeV for the level-1 muon if other signals are available in addition to the muon. After applying the trigger level-1 acceptance, the number of triggered $\mathrm{b\bar{b}}$ events is typically few times $10^{10}$ per year. At the level-2 and at higher trigger levels, the triggers are designed to select specific B-decay channels.

ATLAS and CMS have pixel detectors as the detector element closest to the interaction point, thus providing a good vertex resolution. The large tracking systems enable efficient charged particle reconstruction. In addition, ATLAS has the capability for identifying low-$p_{\mathrm{T}}$ electrons ($p_{\mathrm{T}} > 0.5$ GeV) by using the transition radiation in the TRT, while both experiments can use their electromagnetic calorimeters for identifying soft electrons at somewhat higher $p_{\mathrm{T}}$. The use of the ATLAS TRT for $\pi$/K separation has been investigated recently [49]. The results are very encouraging and would enhance greatly the analysis of the two-hadron decays of B-mesons, however, the results are still to be confirmed at beam tests.

# 6 Detector R&D, prototypes and running experience

## 6.1 Targets and beams

In this conference, first running experience was reported on the PEPII and KEKB asymmetric $\mathrm{e^+e^-}$ beam operation [50], [51]. At KEKB, synchrotron light background from the whole ring was found to be a significant issue for the BELLE operation, requiring further work. At PEPII, the main source of BaBar background was found to be lost particles, coming from local bremsstrahlung, and local or distant Coulomb scattering.

HERA-B experiment has already several years experience on the wire target operation [28]. Two sets of four wires are placed at the beam halo, located at a distance of four to ten standard deviations from the beam. The distance is not constant, but as the beam intensity drops, the wires are brought continuously closer to the beam core to keep a constant interaction rate. Even though the proton beam lifetime is reduced due to the fact that the wire target operation is consuming between 1 and 2 mA/h of the proton current, the luminosity and the background conditions to the other HERA experiments are not affected. A reliable target steering and stable operation have been achieved.

## 6.2 Multilevel triggering

Apart from the $e^+e^-$ B-experiments, the trigger is a vital issue since the fraction of B-events varies from about 1% (LHC) down to $10^{-6}$ (HERA-B). Moreover, since the branching fractions of interesting final states are typically small, the experiments have to have interaction rates $\mathcal{O}(10$ MHz$)$ or more. All the experiments use a multilevel triggering scheme. Some experiments use a pre-trigger (level-0) either to discard empty crossings (HERA-B), or to make a pile-up veto (LHCb). The lowest level physics trigger (level-1) is searching for high-$p_T$ leptons or hadrons. This is achieved in most experiments by using fast trigger detectors stand-alone. Only HERA-B will use tracking in level-1 to confirm the high-$p_T$ hadron signals. BTeV is the only experiment which is planning to use an event topology trigger at level-1, searching for displaced vertices. At the higher trigger levels, data is kept in pipelines for online event processing. Data storage is expected to operate at a 100 Hz rate, apart from BTeV which is planning to compress the data online, and to write out only data summary information.

## 6.3 Tracking and vertexing

Microvertex detectors, located as close to the primary vertex as practically possible, are crucial for precise secondary vertex measurements. In $e^+e^-$ experiments at the $\Upsilon(4S)$, the vertex detectors operate also as stand-alone tracking devices for very low-momentum particles. In forward spectrometer geometries, retractable detector disks are located inside the beam vacuum vessel, while in central experiments the closest detector layer can be placed just outside the beam pipe. Technologies employed are either Si-strip detectors or Si-pixels. Radiation hardness is an issue even for the vertex detectors in $e^+e^-$ experiments – for example the BaBar vertex detector is foreseen to tolerate a 2.4 kGy dose per year, thus guaranteeing a 10-year operation [37]. For comparison, at HERA-B, in the detector area closest to the beam, the maximum dose per year is 100 kGy, and it is foreseen that the silicon detectors will be exchanged once per year [30].

Tracking systems are facing unforeseen operational requirements with the high particle rates. Progress has been made in solving detector physics and chemistry problems at high particle rates. HERA-B experience with the honeycomb drift chambers has given valuable lessons on the careful choice of materials, glues and gases [34]. The problems at HERA-B with a new device, MSGC, are not that surprising since these detectors have never been used before in high-energy physics experiments. While the HERA-B experiment has equipped their MSGCs with GEMs [35], thus achieving satisfactory performance, the CMS experiment is studying using advanced passivation on their MSGCs [52]. In this method, a strip of dielectric material is deposited over all the cathode edges to prevent electron extraction by the high electric field at the strip edges. Using this method, together with high surface resistivity and narrow anodes, the CMS prototype detectors have been proven to operate in an LHC-like radiation environment.

The possibility for $dE/dx$ measurements has proven to be a valuable asset, if no other particle identification method is available and if the momentum spectrum of particles is suitable. It has been used in $e^+e^-$ experiments (CLEO, LEP experiments) as well as in hadronic experiments (CDF).

## 6.4 Calorimetry and muons

The electromagnetic calorimeters are used for triggering electrons and photons, and for reconstructing electrons, photons, and $\pi^0$ and $\eta$ mesons. Different experiments have very different dynamic ranges and radiation hardness requirements, leading to different choices for calorimeters. The $e^+e^-$ experiments (CLEO, BaBar, BELLE) operate at low energies, and the choice has been CsI crystals, which are sensitive down to 10-20 MeV photons. Hadron experiments require a large dynamic range and high radiation hardness. The choice has been either high-resolution crystal calorimeters ($PbWO_4$) in BTeV and CMS, or standard sampling calorimeters with more modest energy resolution (lead-scintillators in LHCb, lead-LAr in ATLAS). The hadron calorimeters play a minor role in B-physics. Nevertheless, they are used for muon identification and as a muon filter, as well as for hadron triggers and for enhancing $K^0_L$ identification in BaBar and BELLE.

Muons represent the cleanest way of tagging B-meson final states, and all experiments are designed to trigger and reconstruct muons with a high efficiency. Some experiments (D0, BTeV, ATLAS) have a powerful stand-alone muon momentum measurement, provided by toroids in the muon system.

## 6.5 Charged hadron identification

Charged hadron identification is a feature which often puts contradictory requirements on the detector, compromising the operation of other detector elements.

Therefore dedicated devices such as Cherenkov counters are only incorporated in experiments which consider physics with identified hadrons as their first priority. This is obviously the case with dedicated B-physics experiments, which all are relying on Cherenkov counters of some sort. In addition, Cherenkov counters are used extensively in heavy-ion and astrophysics experiments. General purpose high-energy physics experiments have to compromise between the requirements on the particle identification on one hand, and on the minimisation of material in front of the calorimeters and maximisation of the tracking volume, on the other hand. Therefore, most general purpose experiments have chosen to have either a $dE/dx$ capability in the tracker (CDF, ATLAS), or no identification at all – among the recent general purpose collider experiments, only DELPHI and SLD have had Cherenkov counters.

Cherenkov counters are the most practical solution for identifying charged hadrons over a large momentum range, typically between 1 and 150 GeV. Relativistic particles emit Cherenkov radiation in a medium. The angle of emission is proportional to the velocity of particle as $\theta = \arccos(1/n\beta)$, where $n$ is the index of refraction. When the angle is measured using photosensitive devices, and the momentum is measured independently in another detector, the mass of the particle can be defined. The choice of radiator medium depends on the desired momentum range for identification, and on the available space. The larger the refractive index, the larger the emission angle, and the radiator can thus be made thinner. On the other hand, large refractive index is correlated with a high density, which is harmful for the operation of other subdetectors. Characteristics of radiators in Cherenkov detectors in B-physics experiments are summarised in Table 1.

| Radiator material | $CF_4$ | $C_4F_{10}$ | Aerogel | LiF | fused silica (quartz) |
|---|---|---|---|---|---|
| $n$ | 1.0005 | 1.0014 | 1.01-1.10 (ref. 1.03) | 1.50 ($\lambda = 150$ nm) | 1.474 |
| $\theta_c^{max}$ [mrad] | 32 | 53 | 242 | 841 | 825 |
| $p_{thr}^{\pi}$ [GeV] | 4.4 | 2.6 | 0.6 | 0.12 | 0.13 |
| $p_{thr}^{K}$ [GeV] | 15.6 | 9.3 | 2.0 | 0.44 | 0.46 |
| State | gas | gas | solid | solid | solid |
| Experiment | LHCb | HERA-B BTeV LHCb | BELLE LHCb | CLEOIII | BaBar |

Table 1: Characteristics of radiators in RICH detectors in B-physics experiments: refractive index $n$, maximum emission angle $\theta_c^{max} = \arccos(1/n)$, and threshold momenta for pions and kaons ($p_{thr} > m/\sqrt{(n^2-1)}$). The state is given for room temperature.

The light collection must be efficient to obtain a sufficient amount of photoelectrons per particle. The detector walls have to have a high transparency for the radiated photon spectrum (walls are typically made of quartz, $CaF_2$, or borosilicate), while the detectors must have a high quantum efficiency [53], [54]. Detectors can be either multiwire chambers with gas doped with TMAE or TEA as the photosensitive component, multiwire chambers with reflective CsI photocathode, standard PMTs, or hybrid photodiodes (HPDs), which combine a photocathode to a small Si-strip or Si-pad drift chamber [55].

The specific ionisation ($dE/dx$) can be used at a more limited momentum range than Cherenkov radiation for charged hadron identification. The minimum of the Bethe-Bloch curve for the specific ionisation is around $\beta\gamma$=3.0-3.5, and the relativistic rise region of $\beta\gamma$ which can be used for particle identification is roughly from 10 to 400, leading to $\pi$/K separation for momenta between 1 and 50 GeV [56]. Moreover, the required detector length is larger than for Cherenkov counters to achieve the same separation. Particle identification by $dE/dx$ is thus a feasible option for B-physics experiments which have a significant fraction of the B-hadron decay products in this momentum range. This is the case for the $e^+e^-$ experiments at the $\Upsilon$(4S), and also the central collider experiments, while at forward experiments the momentum spectrum is harder.

The particle identification technologies used or foreseen for B-physics experiments are summarized in Table 2.

| Experiment | Hadron identification technique | Status |
|---|---|---|
| CDF | $dE/dx$ in COT | ready for RunII |
| | TOF | design, pending funding |
| D0 | - | |
| CLEOIII | LiF RICH, chambers with TEA [40, 62] | being installed |
| BaBar | DIRC [36, 58] | working |
| | $dE/dx$ in DCH | working |
| BELLE | Aerogel | working |
| | TOF | working |
| | $dE/dx$ in CDC | working |
| HERA-B | $C_4F_{10}$ RICH, PMTs [31] | working |
| LHCb | $C_4F_{10}$ and aerogel RICH1 | design |
| | $CF_4$ RICH2 | |
| | readout with HPDs or PMTs [59] | |
| BTeV | $C_4F_{10}$ and aerogel RICH | design |
| ATLAS | $dE/dx$ in TRT | design, pending beamtest verification |
| CMS | - | |

Table 2: Charged hadron identification techniques in different experiments.

The HERA-B RICH detector has proven that a Cherenkov counter can be operated successfully in the harsh forward hadron spectrometer environment [31]. The RICH has been designed to separate pions and kaons in the momentum range between 10 and 75 GeV. The radiator used is $C_4F_{10}$ gas. The photons are imaged by two spherical mirrors and two planar mirrors onto two photon detection systems outside the spectrometer active volume. Due to the very high interaction rate and large multiplicity of charged particles, the Cherenkov photon flux is up to several MHz per cm$^2$, and only photomultipliers were found to operate reliably over the lifetime of the experiment [57]. The photon detectors thus consist of multianode PMTs, with 16 anodes for the inner region and 4 anodes for the outer region to match the expected occupancy. In addition, there is a two-lens telescope in front of each PMT to solve the PMT packing problem and to match the anode dimension to the dispersion error.

The detector was completed in January 1999, and the detector was run under realistic data-taking conditions in May 1999. Raw hits of a typical event are shown in Fig. 10. The rings could be reconstructed in hadronic events. Even without the final tracking, but using a crude momentum estimation by matching the calorimeter clusters with the track angles determined from the RICH and assuming that the particles originate from the target, the correlation between the Cherenkov ring opening angle and the particle momentum for different particle species could be demonstrated.

The BaBar experiment has constructed a particle identification system based on the Detection of Internally Reflected Cherenkov (DIRC) light [58]. The DIRC is a novel concept which uses long, thin, rectangular fused silica bars both as radiators and as light guides to direct the produced light via internal reflection to photodetectors. The design has been constrained by the desired momentum range (700 MeV to 4 GeV), and by the demand of minimising material in front of the electromagnetic CsI calorimeter. In addition, for high luminosity running conditions, the particle identification system must have a fast signal response and be able to tolerate high backgrounds. These boundary conditions are well satisfied by the thin fused silica detector elements (17.25 mm thick). Moreover, the photon detectors can be located outside of the active detector volume. At one end of the detector bars, the Cherenkov image is allowed to expand through a standoff region (Standoff Box) filled with water, which has an index of refraction close to that of fused silica, which minimises the total reflection at the interface of the two materials. The expanded image is then detected in an array of PMTs. The instrumented end is located at the backward direction, since in the asymmetric collisions the final state particles emerge mainly to the forward direction. The dummy ends of the detector bars are covered with mirrors to reflect the photons back to the instrumented end.

At the time of the conference, five detector elements out of the total 12 were installed in BaBar [36]. Cosmic ray data showed a large number of photons collected and a close agreement of the data with Monte Carlo predictions. A

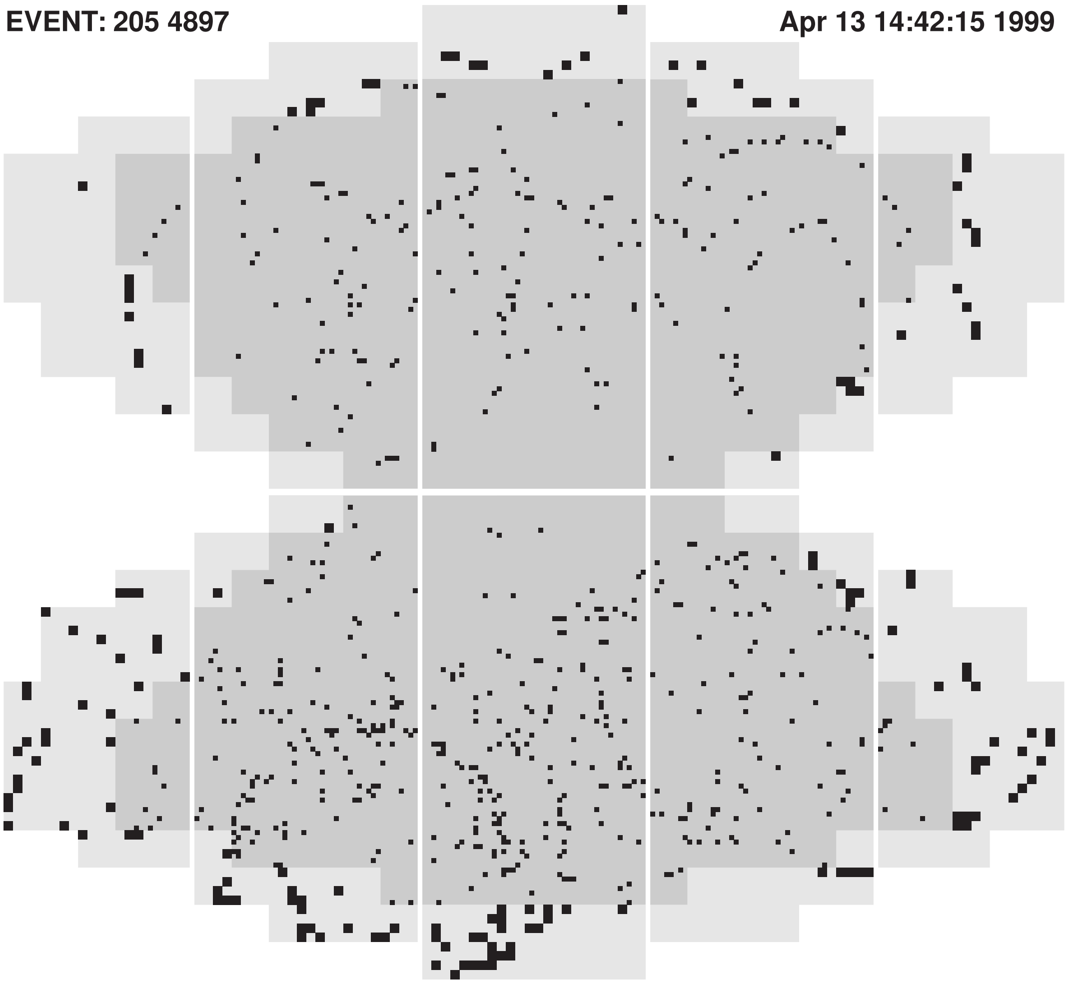


Figure 10: Raw hits of a typical event in the HERA-B RICH [31].

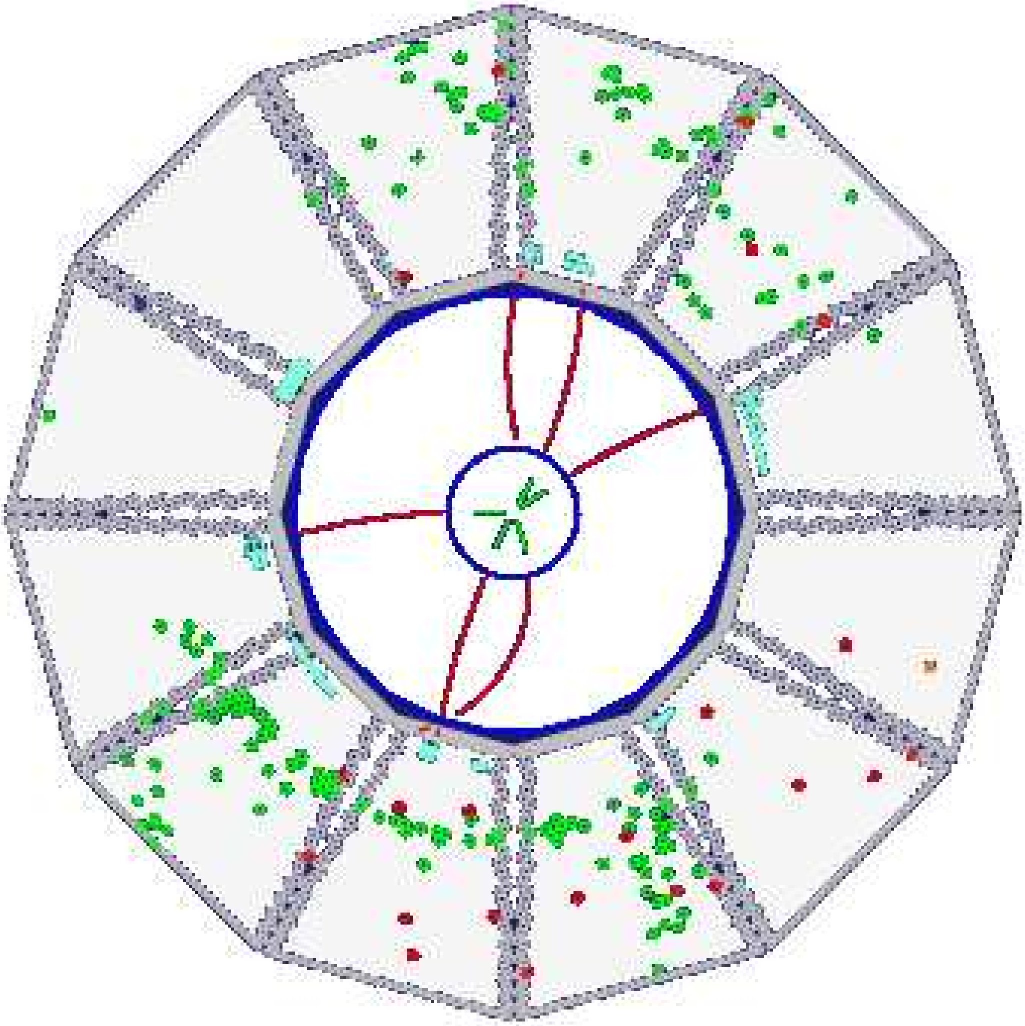

Figure 11: Event display of a multi-hadron event the in the BaBar DIRC [36].

typical multihadron event reconstructed in the DIRC is shown in Fig. 11. The dominant class of background photons originates from the event itself, while beam-related background can be rejected effectively by the good time-resolution of the PMTs. The remainder of the detectors will be installed by end of 1999.

The LHCb experiment has the most difficult task for designing their particle identification system due to the largest momentum range to be covered, from 1 to 150 GeV. This will be accomplished by using two RICH counters, RICH1 with an aerogel and $C_4F_{10}$ radiators, and a RICH2 with a $CF_4$ radiator [59]. At LHCb, however, there is a strong correlation between the particle polar angle and momentum, and therefore the angular coverages of the detectors do not have to be the same. The RICH1 is intended for low momentum tracks and will have 25-300 mrad polar angle coverage. Tilted spherical mirrors will focus the Cherenkov rings to photodetectors outside the detector acceptance. The RICH2 is intended for high momentum, and consequently small polar angle tracks, and it will cover polar angles 10-120 mrad. The Cherenkov photons are reflected with flat mirrors onto spherical mirrors, which will focus the photons to photodetectors. Three photodetector options are presently under study: commercial multianode PMTs, pad HPDs, and pixel HPDs.

# 7 Performance comparison of B-physics experiments

The performance of several B-physics and general purpose experiments is compared in Table 3. The $e^+e^-$ B-factory experiments will collect data in clean conditions, but the performance is limited by statistics and the fact that only $B^0_d/B^+$ mesons can be produced. Presenting the BaBar estimates as an example, and assuming 30 fb$^{-1}$ integrated luminosity, $\sin 2\beta$ will be measured with an accuracy of 0.12 using the $B^0_d \to J/\psi K^0_S$ decays (charged particle final states) – the precision will be improved to about 0.08 combining various other modes. The number of reconstructed, untagged events in the $B^0_d \to \pi^+\pi^-$ final state will be only 64, assuming a branching ratio of $4.7 \cdot 10^{-6}$. Several years of data-taking, and combination of other decay modes will be necessary to obtain reliable information on the angle $\alpha$. The angle $\gamma$ could be studied with the decay mode $B^0_d \to D^{(*)}\pi$ – the statistical accuracy of $\sin(2\beta+\gamma)$ would be 0.22. Using decays $B^\pm \to DK^\pm$ and $B^0_d \to D^0K^*$, 300 fb$^{-1}$ would be needed to obtain a precision in the range 10°-20°. Other possible measurements will be measurements on $|V_{ub}|$ and $|V_{cb}|$, as well as rare decays of the type $B \to K\gamma$. The BELLE performance should be similar to BaBar, and if KEKB will be successful in achieving the design luminosity of $1.0 \cdot 10^{34}$ cm$^{-2}$s$^{-1}$, the BELLE experiment should gain about a factor of three in statistics compared to BaBar.

Hadronic experiments will be more challenging in view of the much smaller signal-to-background ratio. Nevertheless, experience from CDF has already shown the feasibility of achieving significant results in a hadron collider experiment. As we gain more insight on the complicated pattern of CP-violating phenomena, more and more channels will turn out to be important to be experimentally reachable to constrain theoretical uncertainties and to control experimental systematic uncertainties. This leads to the following requirements:

- large statistics,
- access to $B^\pm/B^0_d/B^0_s/B_c/\Lambda_b$ hadrons,
- trigger on purely hadronic final states,
- charged hadron identification.

| Measurement | BaBar BELLE | HERA-B | CDF (D0) | LHCb BTeV | ATLAS CMS |
|---|---|---|---|---|---|
| $\sin 2\beta$ | ** | ** | ** | **** | **** |
| $\delta(\sin 2\beta)$ | 0.08 | 0.12 | 0.08 | 0.011 | 0.012 |
| $\sin 2\alpha$ | * | * | ** | *** | ** |
| $\mathrm{N}(\pi^+\pi^-)$ rec. | 64 unt. | 270 unt. | 4700 unt. | 4600 tagged | 4400 tagged |
| angle $\gamma$ | * $\mathrm{B_d^0} \to \mathrm{D^{(*)}}\pi$, $\mathrm{B^\pm} \to \mathrm{DK^\pm}$, $\mathrm{B_d^0} \to \mathrm{DK^*}$ | | * $\mathrm{B^\pm} \to \mathrm{DK^\pm}$, $\mathrm{B_s^0} \to \mathrm{D_s^- K^+}$ | *** $\mathrm{B_d^0} \to \mathrm{D^{(*)}}\pi$, $\mathrm{B_d^0} \to \mathrm{DK^*}$, $\mathrm{B_s^0} \to \mathrm{D_s^- K^+}$ | |
| $\mathrm{B_s}$ mixing $\Delta m_s$ reach | | * 12 $\mathrm{ps^{-1}}$ | ** 25 $\mathrm{ps^{-1}}$ | **** 51 $\mathrm{ps^{-1}}$ | *** 40 $\mathrm{ps^{-1}}$ |
| $\mathrm{B_s}$ analyses $\delta(\delta\gamma))$ from $\mathrm{B_s} \to \mathrm{J}/\psi\phi$ | | * | ** 0.16 | **** 0.01 | *** 0.03 |
| $\mathrm{B} \to \mu\mu(\mathrm{X})$ | | | | *** | *** |
| Integrated $\mathcal{L}$ | 30 $\mathrm{fb^{-1}}$ | 30 $\mathrm{fb^{-1}}$ | 2 $\mathrm{fb^{-1}}$ | 2 $\mathrm{fb^{-1}}$ | 30 $\mathrm{fb^{-1}}$ |

Table 3: Performance comparison of different experiments. Where applicable, **** indicates a 1% measurement, *** a few% measurement, ** a 10% measurement and * a measurement. The branching ratio for the decay $\mathrm{B_d^0} \to \pi^+\pi^-$ was assumed to be $4.7 \cdot 10^{-6}$ [23]. For the $\mathrm{B_s} \to \mathrm{J}/\psi\phi$ analysis $x_s = 20$ was assumed.

While the HERA-B RICH is proving the feasibility of charged hadron identification in hadronic experiments, the statistics will be the limiting factor of the HERA-B physics programme. After one year of data-taking, it is foreseen that the $\sin 2\beta$ will be measured with an accuracy of 0.13 using the $\mathrm{B_d^0} \to \mathrm{J}/\psi\mathrm{K_S^0}$ decays. The number of reconstructed, untagged events in the $\mathrm{B_d^0} \to \pi^+\pi^-$ final state will be about 270, assuming a branching ratio of $4.7 \cdot 10^{-6}$. The expected background, however, cannot be reliably estimated. The $\mathrm{B_s^0}$ mixing parameter $\Delta m_s$ will be reachable up to about 12 $\mathrm{ps^{-1}}$[60].

CDF (and D0) will be serious competitors for the dedicated B-experiments at the first phase of B-experimentation before the LHC startup. CDF at the RunII will fulfil all the requirements above, while D0 will be lacking hadron identification and hadronic trigger. After two years of data-taking (2 $\mathrm{fb^{-1}}$), CDF expects to measure $\sin 2\beta$ with an accuracy of 0.084 (0.07 with a kaon tag using the TOF). The number of reconstructed, untagged events in the $\mathrm{B_d^0} \to \pi^+\pi^-$ final state will be about 4700, assuming a branching ratio of $4.7 \cdot 10^{-6}$. A $1.3\sigma$ $\pi/\mathrm{K}$ separation is expected for particles with transverse momenta greater than 2 GeV using the $dE/dx$ in the COT, thus helping to extract the signal from the two-body background. CDF has studied possibilities for extracting the angle $\gamma$ by using decays $\mathrm{B^\pm} \to \mathrm{DK^\pm}$ and $\mathrm{B_s^0} \to \mathrm{D_s^- K^+}$, but the preliminary studies indicate a poor accuracy. The decay mode $B_s^0 \to J/\psi\phi$ will be experimentally easy, and observing an asymmetry in this decay mode would signal the existence of an anomalous CP violating phase. The parameter $\delta\gamma$ can be measured with a precision of 0.16 ($x_s = 20$). The $B_s^0$ mixing parameter $\Delta m_s$ will be reachable up to about 25 ps$^{-1}$ with the CDF baseline detector (20 000 signal events, signal-to-background ratio of 1:2).

The dedicated B-experiments LHCb at LHC and BTeV at Tevatron are being designed to fulfil all the requirements above in an optimal way. After one year of data-taking (2 fb$^{-1}$), the LHCb experiment will have measured $\sin 2\beta$ with an accuracy of the order of 1%. The number of reconstructed and tagged events in the $B_d^0 \to \pi^+\pi^-$ final state will be about 4600, assuming a branching ratio of $4.7 \cdot 10^{-6}$. Various modes for extracting the angle $\gamma$ are being investigated – here it will be mandatory to use the full power of the charged hadron identification. The $B_d^0 \to D^0 K^*$ modes will yield a precision of order 10° for the angle $\gamma$. The decay mode $B_d^0 \to D^{(*)}\pi$ will need five years running to get the precision on $2\beta + \gamma$ down to 4°. The $B_s^0 \to D_s^- K^+$ decay mode will allow measuring $\gamma - 2\delta\gamma$ with a statistical precision between 6° and 13° with one year's data, depending on the numerical values of the parameters involved. The parameter $\delta\gamma$ can be measured with a precision of 1% in one year using decays $B_s^0 \to J/\psi\phi$ and the $B_s^0$ mixing parameter $\Delta m_s$ will be reachable up to about 51 ps$^{-1}$. Rare decays of the type $B \to K^{*0}\gamma$ can be reconstructed efficiently.

Compared to the LHCb performance, the BTeV experiment has actually some advantages despite of the apparent handicap of smaller center-of-mass energy, resulting in quite similar expectations for the physics reach. The longer bunch-spacing and the longer interaction region allow accepting multiple interactions. Smaller boost means that the experiment can be made shorter and further away from the beam, saving from radiation damage. If the two-arms and the vertex trigger can be realised this is an obvious big advantage.

The general purpose experiments ATLAS and CMS at LHC will be competitive with the dedicated experiments in some channels. In addition, if some charged particle identification can be realised, the spectrum of the B-physics programme can be made much wider. ATLAS and CMS are expected to obtain a very good precision for the measurement of $\sin 2\beta$, at the level of 1% with 30 fb$^{-1}$. Various parameters of the $B_s^0$-meson system will be measured for example with $B_s^0 \to D_s\pi, D_s a_1$, and $B_s^0 \to J/\psi\phi$ final states [61]. The $B_s^0$ mixing parameter $\Delta m_s$ will be reachable up to about 40 ps$^{-1}$, and the statistical precision for $\delta\gamma$ will be about 3% ($x_s = 20$). There are some hopes for the angle $\alpha$ measurement – in ATLAS, a $\pi/K$ separation is expected to be possible at the one-standard-deviation level using the TRT. The issue is to be verified with beam test data. The number of reconstructed and tagged events in the $B_d^0 \to \pi^+\pi^-$ final state will be about 4400, assuming a branching ratio of $4.7 \cdot 10^{-6}$. Various other precision measurements such as B-baryon lifetimes and polarizations will be feasible. Rare decays of the type $B \to \mu\mu(X)$ are particularly suitable for ATLAS and CMS since they are self-triggering, and the high-luminosity data of LHC can be used as well. For example, the decay mode $B_s^0 \to \mu^+\mu^-$, for which the SM branching fraction is $3.5 \cdot 10^{-9}$, should be observed.

# 8 Conclusions

We are living exciting times. The first direct measurement of an angle of the Unitarity Triangle has emerged from CDF when the physicists have learned to use the limited statistics in an optimal way. Meanwhile, the precision measurements from CLEO, LEP, SLD, CDF and kaon experiments are constraining more and more the Unitarity Triangle. The first generation of B-physics experiments is getting off the ground and hoping to get to a cruising speed soon, while the Tevatron experiments are expected to continue producing even more exciting results in the coming run. From years of planning, designing and reviewing experiments we are now getting into the experimentation itself, and hopefully already in the next BEAUTY conference new results can be reported.

It is also important to discuss the future developments. Therefore, the future projects at LHC and at Tevatron have their due place in this conference. When we learn more about B physics, the experiments can be better optimised to cover fully the physics spectrum, while new ideas, technological progress and experience help us to design better particle detectors.

# 9 Acknowledgements

Thanks to Peter Krizan and other local organizers for a well-organized conference in a beautiful location, to Peter Schlein and Samim Erhan for making and keeping up the spirit of this conference series, to all the conference participants for an interesting and enjoyable week, and to all the authors of the contributed papers for providing me with the material for this summary.

# References


[1] M. Calvetti, these proceedings.

[2] D. Wyler, these proceedings.

[3] R. Fleischer, these proceedings.

[4] D. Pirjol, these proceedings.

[5] H. Lipkin, Y. Nir, H. Quinn and A. Snyder, Phys. Rev. D44 (1991) 1454.

[6] P.F. Harrison (ed.) *et al.*, BaBar Collaboration, 'The BaBar Physics Book: Physics at an Asymmetric B Factory', SLAC-R-0504, Oct. 1998.

[7] M. Gronau and D. London, Phys. Rev. Lett. 65 (1990) 3381.

[8] R. Aleksan, I. Dunietz and B. Kayser, Z. Phys. C54 (1992) 653.

[9] I. Dunietz, Phys. Lett. B270 (1991) 75.

[10] M. Gronau and D. Wyler, Phys. Lett. B265 (1991) 172.

[11] R.G. Sachs, EFI-85-22 (1985) (unpublished);
I. Dunietz and R.G. Sachs, Phys. Rev. D37 (1988) 3186;
I. Dunietz, Phys. Lett. B427 (1998) 179.

[12] O. Schneider, these proceedings.

[13] R. Fleischer, Phys. Lett. B365 (1996) 399;
R. Fleischer and T. Mannel, Phys. Rev. D57 (1998) 2752;
M. Gronau and J. Rosner, Phys. Rev. D57 (1998) 6843.

[14] M. Gronau, J. Rosner and D. London, Phys. Rev. Lett. 73 (1994) 21;
M. Neubert and J. Rosner, Phys. Lett. B441 (1998) 403 and Phys. Rev. Lett. 81 (1998) 5076.

[15] A. Buras and R. Fleischer, CERN-TH/98-319 (1998), hep-ph/9810482, to appear in Eur. Phys. J. C.

[16] H.G. Moser and A. Roussarie, Nucl. Instrum. and Methods A384 (1997) 491.

[17] P. Maksimovic, these proceedings.

[18] K. Ackerstaff *et al.*, OPAL Collaboration, Eur. Phys. J. C5 (1998) 379.

[19] K. Berkelman, 'CLEO results', these proceedings.

[20] Y. Rozen, F. Pierre and G. Calderini, these proceedings.

[21] LEP $V_{cb}$ working group results for the Tampere EPS-HEP Conference, July 1999.

[22] LEP B-oscillation working group results for the Stanford Lepton-Photon Conference, August 1999.

[23] D.E. Jaffe, CLEO Collaboration, talk given at the 8$^{\rm th}$ International Symposium on Heavy Flavour Physics, Southampton, 25-29 July 1999.

[24] F. Parodi, P. Roudeau and A. Stocchi, Il Nuovo Cimento Vol. 112 A, N. 7 (1999).

[25] S. Mele, Phys. Rev. D59 (1999) 113011.

[26] A. Ali, 'Precision Flavour Physics and Supersymmetry', DESY 99-083, UdeM-GPP-TH-99-60, hep-ph/9907243, July 1999.

[27] C. Padilla, these proceedings.

[28] K. Ehret, these proceedings.

[29] E.K.E. Gerndt and S. Xella, these proceedings.

[30] W. Wagner, these proceedings.

[31] J. Pyrlik, these proceedings.

[32] A. Zoccoli, these proceedings.

[33] M. Titov, these proceedings.

[34] M. Capeans, these proceedings.

[35] T. Zeuner, these proceedings.

[36] A. Hoecker, these proceedings.

[37] S. McMahon, these proceedings.

[38] T. Iijima and E. Prebys, these proceedings.

[39] K. Berkelman, 'The Future CESR-CLEO Program', these proceedings.

[40] G. Viehhauser, these proceedings.

[41] V. Papadimitrou, these proceedings.

[42] A. Lucotte, these proceedings.

[43] S. Amato *et al.*, LHCb Collaboration, LHCb Technical Proposal, CERN LHCC 98-4, LHCC/P4 (1998).

[44] A. Kulyatsev *et al.*, BTeV Collaboration, BTeV Preliminary TDR, BTeV-Pub-99/2, submitted to Fermilab PAC May 1999.

[45] R. Gardner, these proceedings.

[46] A. Airapetian *et al.*, ATLAS Collaboration, ATLAS Detector and Physics Performance Technical Design Report Vol II, CERN/LHCC/99-15, ATLAS TDR 15 (1999).

[47] R. Jones, these proceedings.

[48] A. Starodumov, these proceedings.

[49] D. Barberis, these proceedings.

[50] W. Kozanecki, these proceedings.

[51] T. Iijima, these proceedings.

[52] G. Flugge *et al.*, these proceedings.

[53] J. Seguinot and T. Ypsilantis, Nucl. Instrum. and Methods A433 (1999) 1.

[54] T. Ekelöf, Nucl. Instrum. and Methods A433 (1999) 372.

[55] P. Weilhammer, these proceedings.

[56] For a recent review see for example B. Dolgoshein, Nucl. Instrum. and Methods A433 (1999) 533.

[57] P. Krizan *et al.*, Nucl. Instrum. and Methods A394 (1997) 27.

[58] I. Adam *et al.*, Nucl. Instrum. and Methods A433 (1999) 121.

[59] A. Go, these proceedings.

[60] I. Abt, Nucl. Instrum. and Methods A384 (1996) 113;
T. Lohse, Nucl. Instrum. and Methods A408 (1998) 154.

[61] M. Smizanska, these proceedings.

[62] R. J. Mountain *et al.*, Nucl. Instrum. and Methods A433 (1999) 77.